New mucosal bivalent live-attenuated vaccine is protective against Human Metapneumovirus and Respiratory Syncytial Virus

Daniela Ogonczyk-Makowska, Clémence Vacher, Andrés Pizzorno, Pauline Brun, Caroline Chupin, Clément Droillard, Julie Carbonneau, Emilie Laurent, Victoria Dulière, Aurélien Traversier, et al.

Article

New mucosal bivalent live-attenuated vaccine is protective against Human Metapneumovirus and Respiratory Syncytial Virus

Daniela Ogonczyk-Makowska[1, 2], Clémence Vacher[1, 2, 3], Andrés Pizzorno[2, 3, 4], Pauline Brun[2, 3, 4], Caroline Chupin[2, 3, 5], Clément Droillard[2, 3, 4], Julie Carbonneau[1, 2], Emilie Laurent[2, 3, 4], Victoria Duliere[2, 3, 4], Aurélien Traversier[2, 3, 4], Olivier Terrier[2], Thomas Julien[2, 3, 4], Marie Galloux[6], Stéphane Paul[7], Jean-François Eléouët[6], Marie-Eve Hamelin[1, 2], Guy Boivin[1, 2*], Manuel Rosa-Calatrava[2, 3, 4*] and Julia Dubois[2, 3, 4, 5*]

[1] Centre de Recherche en Infectiologie of the Centre Hospitalier Universitaire de Québec and Université Laval, QC G1V 4G2, Canada; daniela.ogonczyk-makowska@crchudequebec.ulaval.ca

[2] International Associated Laboratory RespiVir (LIA VirPath-LVCM France-Canada), 18 Université Laval, QC G1V 4G2, Québec, Canada, Université Claude Bernard Lyon 1, Université de Lyon, 69008 Lyon, France; manuel.rosa-calatrava@univ-lyon1.fr, guy.boivin@crchudequebec.ulaval.ca

[3] CIRI, Centre International de Recherche en Infectiologie, Team VirPath, Univ Lyon, 14 Inserm, U1111, Université Claude Bernard Lyon 1, CNRS, UMR5308, ENS de Lyon, F-15 69007, Lyon, France; julia.dubois@univ-lyon1.fr

[4] VirNext, Faculté de Médecine RTH Laennec, Université Claude Bernard Lyon 1, Université de Lyon, 69008 Lyon, France, manuel.rosa-calatrava@univ-lyon1.fr

[5] Vaxxel, 43 Boulevard du onze novembre 1918, 69100, Villeurbanne, France;

[6] Université Paris-Saclay, INRAE, UVSQ, VIM, 78350 Jouy-en-Josas, France; marie.galloux@inrae.fr, jean-francois.eleouet@inrae.fr

[7] CIRI, Centre International de Recherche en Infectiologie, Team GIMAP, Univ Jean Monnet Saint-Etienne, CIC Inserm 1408, 14 Inserm, U1111, Université Claude Bernard Lyon 1, CNRS, UMR5308, ENS de Lyon, F-15 69007, Lyon, France; stephane.paul@chu-st-etienne.fr

SUMMARY.

Live-Attenuated Vaccines (LAVs) stimulate robust mucosal and cellular responses and have the potential to protect against Respiratory Syncytial Virus (RSV) and Human Metapneumovirus (HMPV), the main etiologic agents of viral bronchiolitis and pneumonia in children. We inserted the RSV-F gene into the a HMPV-based LAV (Metavac®) we previously validated for protection of mice against HMPV challenge, and rescued a replicative recombinant virus (Metavac®-RSV), exposing both RSV- and HMPV-F proteins at its surface and expressing them in reconstructed human airway epithelium models. When administrated to BALB/c mice by intranasal route, bivalent Metavac®-RSV demonstrated its capacity to replicate with reduced lung inflammatory score and to protect against both RSV and lethal HMPV challenges in vaccinated mice while inducing strong IgG and broad RSV and HMPV neutralizing antibody responses.

Altogether, our results showed the versatility of Metavac® platform and suggested that Metavac®-RSV is a promising mucosal bivalent LAV candidate to prevent pneumovirus-induced diseases.

Keywords: RSV; HMPV; chimeric virus; bivalent vaccine; live attenuated vaccine; vectored vaccine; reverse genetics; gene insertion; respiratory viruses; pneumovirus; bronchiolitis

---

Abstract Count: 150 words
Figures: 7
Supplementary figures: 2
Intro : 1014 words
Results & discussion : 3808 words
Legends : 1443 words

INTRODUCTION

Human Respiratory Syncytial Virus (RSV) and Human Metapneumovirus (HMPV) are two ubiquitous seasonal human pneumoviruses that cause frequent upper and lower respiratory tract infections (RTIs) throughout the globe [1]. Indeed, RSV infects more than 33 million people/year worldwide resulting in more than 3 million hospitalizations with half occurring in infants under 6 months of age [1,2]. It is the main etiological agent of bronchiolitis and pneumonia in children younger than 1 year [1,3], and causes up to 100 000 deaths in children under the age of 5 [2]. This virus also constitutes an important health problem for adults over 60 and those with risk factors such as immunosuppression or pre-existing heart or lung diseases [4–6]. The other human pneumovirus, HMPV, is also a significant threat in the infant population, with more than 90% of children infected during their first 5 years of age [7]. It is responsible for 5 to 15% of hospitalizations following an acute lower respiratory tract infection [8], and particularly affects children between 1 and 3 years of age [9,10]. On the other hand, HMPV has been identified in 5 to 10% of adults or elderly people with an acute respiratory tract infection and in 3 to 5% of adults having an exacerbation of chronic lung disease or community acquired pneumonia [11,12]. In the US, the hospitalization rate for adults over 65 was reported to be 22 per 10,000 for HMPV, which is similar to RSV with a rate of 25 per 10,000 [11].

Besides symptomatic measures (administration of oxygen or mechanical ventilation and bronchodilators/corticosteroids), there are few specific prophylactic therapies such as Palivizumab (Synagis®), a human monoclonal antibody against the RSV-F protein that can be administered to high-risk infants to prevent severe forms of infection [13,14]. A new human monoclonal antibody with extensive half-life, Nirsevimab (Beyfortus®) [13,15], has been recently licensed by the European Medicines Agency for RSV prophylaxis in newborns. Other types of therapeutic agents (fusion inhibitor peptides, small molecules inhibiting viral polymerase, immunomodulators), are currently in preclinical and clinical development [16,17]. The high prevalence of pneumovirus infections combined with the health and economic burden constitute a major public health challenge in the face of current limited therapeutic arsenal; as such, the WHO considers the development of vaccines against RSV virus as a priority [18].

Research on RSV vaccine field was considerably slowed down by safety concerns in the 1960's; the administration of formalin-inactivated RSV vaccine led to enhanced pulmonary disease (EPD) in vaccinated infants upon subsequent RSV infection [19,20]. Moreover, natural infection with pneumoviruses leads to transient and non-protective immunity [21] and reinfections occur throughout life [22], with both RSV and HMPV having developed intrinsic strategies to counteract or skew host's immune responses [23–27]. More than 20 vaccine candidates against RSV are currently in clinical development [13,28–30], including subunit vaccines, particle-based vaccines, chimeric viruses, mRNA, vector-

based and Live Attenuated Vaccines (LAVs). While the development of an Ad26 vector-based vaccine candidate was recently discontinued following phase III results [13,28,29], the FDA approved in May 2023 the GSK's adjuvanted subunit vaccine (Arexvy®) as the first vaccine to prevent severe RSV disease in the elderly [31]. The pivotal phase III clinical trial reported that vaccination with the stabilized pre-fusion F protein reduced the risk of people 60 and older developing lower respiratory tract disease from RSV by 82.6% and the risk of developing severe disease by 94.1% [32].

One of the limitations of such an intramuscularly (IM)-delivered vaccine resides in its poor capacity to induce a protective mucosal immune response able to block the transmission of respiratory viruses. With this objective, LAVs against respiratory viruses administrated by intranasal (IN) route are considered as a strategy of choice for the pediatric population [33], as they mimic natural viral infection while eliciting robust mucosal and cellular responses without requiring adjuvant [33,34]. Moreover, IN-delivered LAVs offer several advantages over IM-administered vaccines, being easy to use, non-invasive, and more adapted for mass vaccination. About ten LAV candidates against RSV are currently in clinical development and three of them have progressed to phase 2 evaluation [13,30]. Attenuation was achieved by deletion or modification of the NS2, SH, G or M2-2 genes, and/or inserting temperature sensitivity mutations in L gene [13,35–40]. Several evaluations of LAV candidates confirmed the safety of this vaccine stratregy, without associated enhanced respiratory disease; however, variable immunogenicity (neutralizing antibody and mucosal IgA responses) and duration of protection have been reported. Furthermore, the pre-existing serology status of adults and children can affect the clinical outcomes [13,37–39,41–46]. No LAVs against HMPV are currently in clinical development, but some attenuated viruses with G and/or SH gene deletions have shown the potential to progress towards clinical stages [36,38,47–49].

We have previously developed a LAV platform (Metavac®) based on a recombinant HMPV A1/C-85473 strain expressing an endogenous hyperfusogenic F protein and attenuated by deletion of its SH gene (ΔSH-rC-85473-GFP) [50,51]. We provided evidence that such a deletion in the C-85473 backbone prevents the virus-induced activation of NLRP3-inflammasome and subsequently reduces lung inflammation and attenuates pathogenicity in HMPV-infected mice [50,52]. We also described that vaccination of mice with Metavac® confers protection against lethal homologous HMPV A challenge, stimulates induction of neutralizing antibody responses against homologous and heterologous HMPV strains and reduces lung inflammatory response without noticeable markers of enhanced disease [50].

In this context, we re-engineered the Metavac® LAV candidate by reverse genetics and rescued a replicative bivalent attenuated virus (Metavac®-RSV) expressing a native fusion protein of RSV A2 (RSV-F) in addition to its own HMPV-F. Transmission electron microscopy, immunostaining and flow cytometry assays confirmed the efficient expression of both RSV and HMPV-F proteins at the virus surface, in infected monolayers of LLC-MK2 cells and in human airway epithelium (HAE) model. This prompted us to administrate Metavac®-RSV to BALB/c mice by IN route to evaluate its capacity to induce neutralizing antibody responses and protection against RSV A and lethal HMPV A challenges. Our results suggest that Metavac® is a versatile LAV platform and that Metavac®-RSV is a promising mucosal bivalent LAV candidate to prevent bronchiolitis and severe pneumonia induced by pneumoviruses.

RESULTS

Rescue and in vitro characterization of the bivalent Metavac®-RSV virus

After reporting the advantageous properties of the Metavac® (ΔSH-C-85473 HMPV-GFP) recombinant virus and its potential as a LAV candidate against HMPV A and B strains [50], we sought to enlarge the protective scope of this vaccine platform by adding the expression of the exogenous RSV-F antigen. To generate such a recombinant virus by reverse genetics, we inserted the coding sequence of RSV A2 fusion protein into the intergenic region between F and M2 genes in the pSP72 plasmid containing the complete antigenome sequence of Metavac®, as detailed in **Figure 1A**. Insertion in the F/M2 junction resulted in the rescue of a replicative virus (Metavac®-RSV) that was successfully amplified by passages in LLC-MK2 cells.

By using transmission electron microscopy (TEM), we showed that the virus suspension contained pleiomorphic particles covered with glycoproteins, similar to the Metavac® virus (**Figure 1B**). Using dual immunogold labelling, we then showed that the RSV-F protein was detectable at the surface of Metavac®-RSV virions, in addition to endogenous HMPV proteins (**Figure 1B**), demonstrating that the insertion of RSV-F ORF resulted in efficient gene expression, protein production and, ultimately, to the embodiment of the RSV-F protein into the membrane of infected cells with budding viral particles. We then characterized the daily growth kinetics of the Metavac®-RSV virus in LLC-MK2 cells over a 7-day period (**Figure 1C**). In comparison to Metavac® virus, which peaked at 6 ± 0.33 log10 TCID50/ml after 3 dpi, the Metavac®-RSV virus had a slower viral replication, reaching a peak of 5.44 ± 0.09 log10 TCID50/ml after 5 dpi (**Figure 1C**).

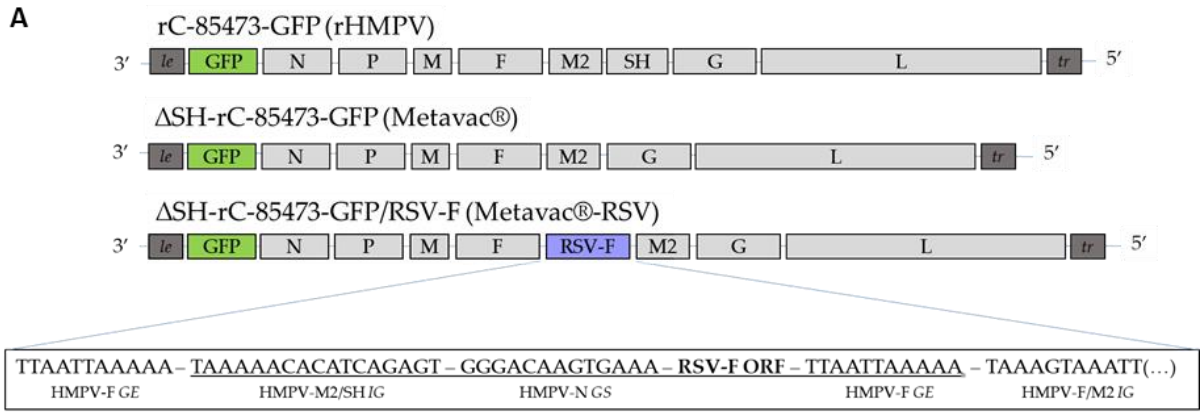

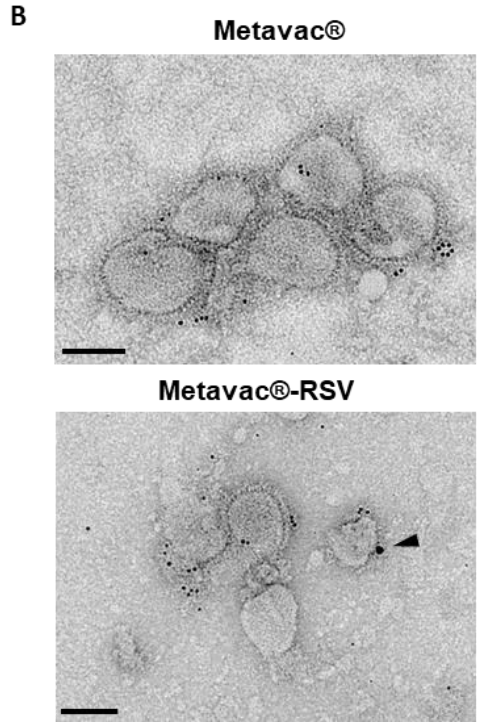

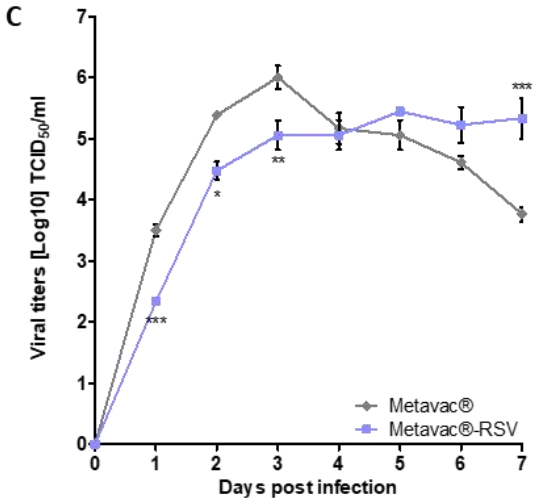

Figure 1. Rescue and characterization of recombinant Metavac®-RSV virus.

(A) Schematic genomic organization of the recombinant HMPV strain (rC-85473-GFP, rHMPV), monovalent Metavac® (ΔSH-rC-85473-GFP) and bivalent Metavac®-RSV (ΔSH-rC-85473-GFP/RSV-F) viruses is represented and the insertion site of the RSV-F ORF between HMPV-F and M2 genes in Metavac®-RSV genome is detailed. GS - Gene Start, GE - Gene End, IG - intergenic sequence. Sequences added to ΔSH-rC-85473-GFP genome are underlined. Genomic sequence is presented from 3′ to 5′ extremity. (**B)** After viral rescue, *in vitro* expression of the RSV-F protein at the surface of Metavac®-RSV viral particles was visualized by transmission electron microscopy after immunogold labelling with anti-HMPV serum (5 nm bead) and the Palivizumab (15 nm bead, black arrowhead) Scale bar = 100nm. (**C)** Viral replication kinetics of the Metavac®-RSV virus were measured in LLC-MK2 cells and compared to the monovalent Metavac® counterpart. Over a 7-day period, culture supernatants were harvested and titrated in TCID50/ml. Results represent the mean of 3 experimental replicates for each time-point. * $p< 0.05$, ** $p < 0.01$, *** $p < 0.001$ when comparing Metavac®-RSV to Metavac® virus using repeated measures two-way ANOVA.

To further investigate the expression of both endogenous HMPV-F and exogenous RSV-F fusion proteins on the cell surface of infected LLC-MK2 cells, we performed co-immunostaining to visualize and quantify those antigens by confocal fluorescent microscopy and flow cytometry. Expression of GFP reporter protein showed that the Metavac®-RSV virus harbored a hyperfusogenic phenotype (**Figure 2A**), according to previous studies with the viral C-85473 background [53,54]. Co-immunostaining with anti-RSV-F (Palivizumab) and anti-HMPV-F (HMPV24) mAbs confirmed the co-expression of the RSV-F protein together with that of HMPV-F by infected cells. When focusing on multinucleated cells at 3 dpi, merged fluorescent signal suggested that RSV-F and HMPV-F proteins were colocalized (**Figure 2A**). To quantify the level of expression of RSV-F at the cell surface of infected LLC-MK2 cells, we performed flow cytometry using Palivizumab and HMPV24 mAbs and detected the presence of both antigens at the cell surface 48 h post-infection (**Figure 2B**). We confirmed that 51.5% of the cells infected with Metavac®-RSV co-expressed both HMPV-F and RSV-F proteins at their surface, whereas 39.6% and 1.5% of infected cells only expressed HMPV-F or RSV-F proteins, respectively (**Figure 2B**). As a comparison, 96.2 % of cells infected with Metavac® only expressed HMPV-F protein at their surface.

These results confirm that more than half of Metavac®-RSV infected cells expressed and exposed on their surface the RSV-F protein, along with the endogenous HMPV-F protein. Altogether, it suggests that the insertion of the RSV A2 F coding sequence into the Metavac® genome is viable and results in the production of a fully functional and replicative bivalent Metavac®-RSV virus.

Figure 2. Co-immunostaining of HMPV and RSV-F glycoproteins in infected LLC-MK2 cells.
(A) LLC-MK2 cells were infected with GFP-expressing Metavac®, Metavac®-RSV or RSV (rRSV-GFP) viruses, fixed and stained at 3 dpi with Palivizumab (red), HMPV24 mAb (white) and DAPI (blue). Merged fluorescent signals are represented (yellow). Images of representative cytopathic effects (CPEs) were taken using Zeiss880 confocal microscope (40x magnification) and processed with ImageJ software. A numeric focus was made on CPEs (square) and presented in the right panel. (**B)** LLC-MK2 cells were infected with MOI 0.5 of either Metavac® (a-e) or Metavac®-RSV (f-j), and antigens expression on the surface of the infected cells was measured by flow cytometry 48h post-infection. HMPV-F protein was detected with HMPV24 mAb conjugated with Alexa Fluor™ 647 and RSV-F protein was detected with Palivizumab conjugated with R-Phycoerythrin. Cells were sorted and analyzed by LSR II Flow Cytometer (BD biosciences®). Approximately 30,000 single live cells were counted per each sample performed in triplicate. The figure shows representative gating of sub-populations on one of the three samples. (a,f) - all cells in the sample; (b,g) – single cells (c,h) – single live cells (d,i) – single live cells positive or negative for GFP expression (e, j) - the percentage of GFP-expressing infected single live cells with HMPV-F expression revealed by HMPV24 mAb and RSV-F expression revealed by Palivizumab.

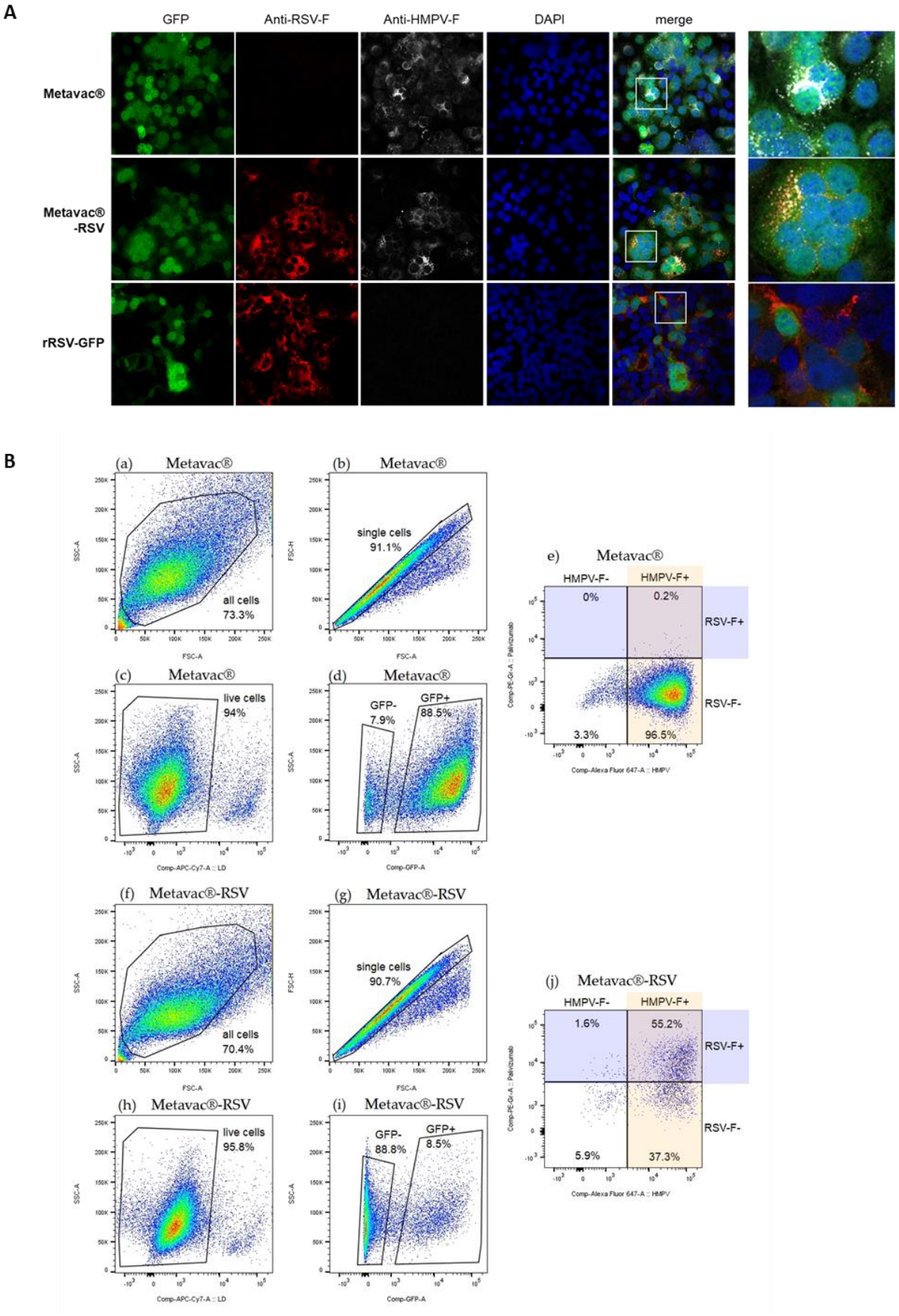

Figure 2. Co-immunostaining of HMPV and RSV-F glycoproteins in infected LLC-MK2 cells.

Bivalent Metavac®-RSV virus is replicative and expresses the RSV-F protein in human airway epithelium model

We further assessed the properties of the bivalent Metavac®-RSV virus to infect and replicate in reconstituted human airway epithelium (HAE). Indeed, we previously showed that Metavac® behaves very similarly to its non-ΔSH rHMPV counterpart, mimicking the in vivo host respiratory epithelium response to such infection [50]. In line with these results, we observed that Metavac®-RSV virus was still infectious and spread within HAE model, as illustrated by the propagation of the GFP signal during a 7-day replication kinetics (**Figure 3A**), which appeared somewhat slower than the propagation of the Metavac® virus (**Figure 3A**). To confirm the delay observed by fluorescent microscopy, we measured the peak number of HMPV-N gene copies at 3 dpi for Metavac® (2.72×10^8) and at 5 dpi for Metavac®-RSV (2.26×10^8) (**Figure 3B**). In accordance with our previous results, we also demonstrated that the Metavac®-RSV virus expressed its exogenous RSV-F gene in an amplification pattern concomitant to the HMPV-N gene expression, reaching a peak of 2.14×10^8 number of RSV-F gene copies per apical wash at 5 dpi (**Figure 3C**).

We then questioned whether and where was the expression of the exogenous RSV-F protein localized within the infected HAE. We thus performed immunofluorescence staining of both RSV-F and HMPV-N proteins at 3 dpi (**Figure 3D**). In accordance with our knowledge of the pneumovirus replication cycle [50,51,55,56], we observed in Metavac®-infected HAE that the HMPV-N protein was localized in large areas into the cytoplasm of ciliated cells, presumably inclusion bodies corresponding to viral replication, as well as into the cilia, where new virions bud from the cell membrane (**Figure 3D**). When infected with Metavac®-RSV, ciliated cells positive for HMPV-N expression also expressed the RSV-F protein, mainly localized into the apical ciliated surface and into smaller cytoplasmic speckles, similar to what was observed when HAEs were infected with rRSV-GFP virus (**Figure 3D**).

These results indicate that Metavac®-RSV harbors attenuated replicative properties in HAE (**Figure 3**), as well as in LLC-MK2 cells (**Figure 1**), in contrast to its monovalent Metavac® counterpart. However, we confirmed that Metavac®-RSV is characterized by efficient infection, replication, and protein expression within the HAE model, leading to further investigation of its potential as a bivalent LAV candidate *in vivo*.

Figure 3. Viral replication and RSV-F expression in human airway epithelium (HAE) model. Reconstituted HAE were infected with Metavac® or Metavac®-RSV viruses at an MOI of 0.1 and monitored for 7 days. (**A**) Viral spread in HAE was monitored at 3, 5 and 7 dpi by GFP fluorescence observation (10× magnification). (**B-C**) Viral quantification from epithelium apical washes collected after 1, 3, 5 and 7 dpi was performed byRT-qPCR targeting the HMPV-N gene (**B**) or the RSV-F gene (**C**). Data are shown as means ± SD and represent experimental triplicates. Dotted line represents the RT-qPCR quantification threshold. ** $p < 0.01$ when comparing Metavac®-RSV to Metavac® virus using repeated measures two-way ANOVA. (**D**) Co-immunostaining of HMPV-N and RSV-F proteins was realized at 3 dpi. Fixed HAE infected by Metavac®, Metavac®-RSV or rRSV-GFP viruses were stained with mixture of mAbs specific to the HMPV-N protein (mAb hMPV123, green), RSV-F protein (Palivizumab, red) and with DAPI (blue) specific to the nucleus. Acquisition of images of representative infected area was performed with confocal inverted microscope (Zeiss Confocal LSM 880) and processed with ImageJ software. Scale bar = 20µm. A focus on apical surface of ciliated infected cells was made (square) and is presented in the right panel.

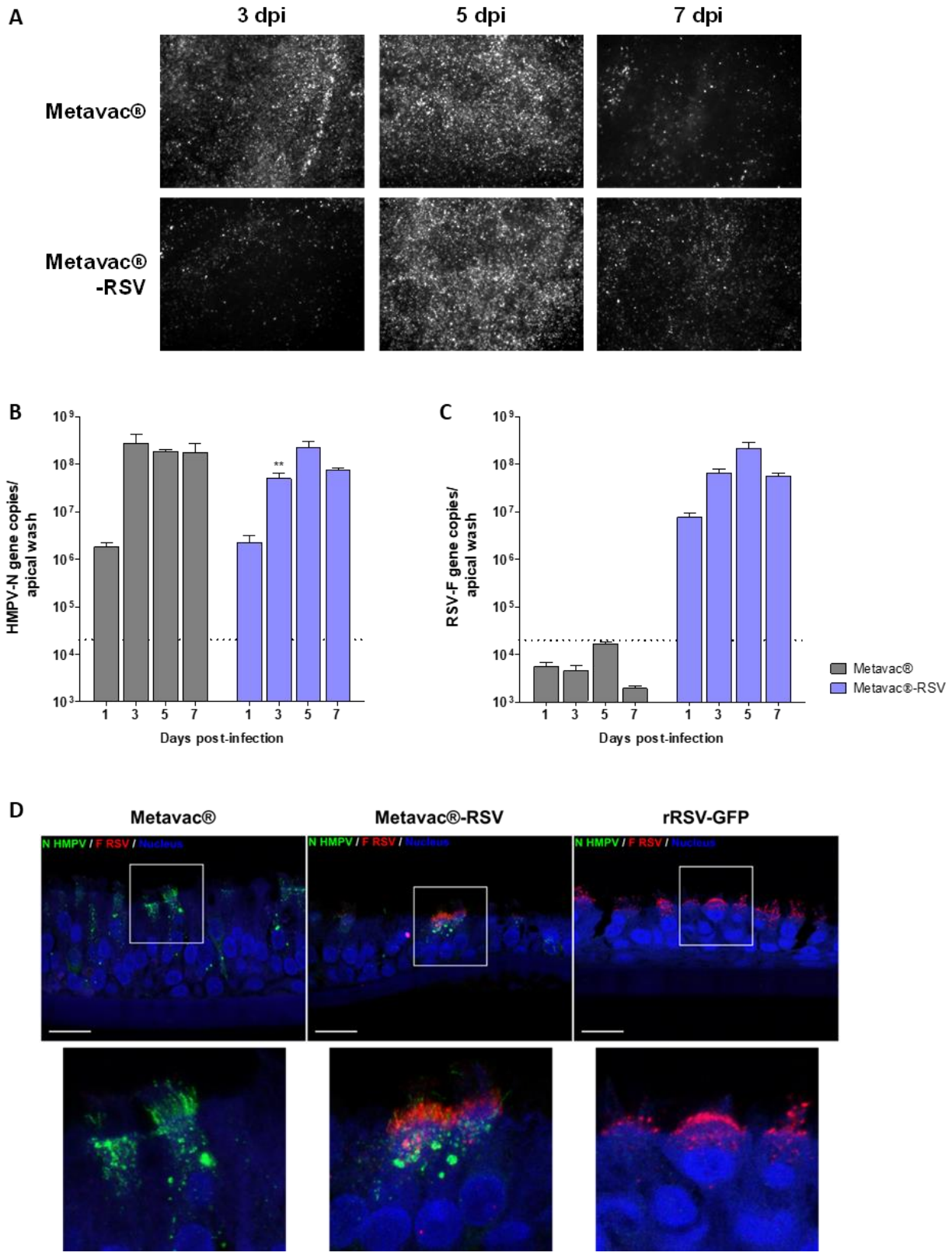

Figure 3. Viral replication and RSV-F expression in human airway epithelium (HAE) model..

Infectivity and attenuation of Metavac®-RSV vaccine candidate in BALB/c mice

To ascertain the level of the Metavac®-RSV attenuation *in vivo*, we infected BALB/c mice by the IN route with 5×10^5 TCID50 of either rHMPV, Metavac® or Metavac®-RSV viruses. This represents a non-lethal dose shown to induce significant weight loss after rHMPV infection but not with Metavac® infection. Similar to the mock (non-infected) group control and contrarily to the rHMPV virus, neither weight loss nor clinical signs were observed when mice were infected with the Metavac®-RSV vaccine candidate during the 14-day follow-up (**Figure 4A**).

Two days after IN instillation, we measured the quantity of viral genome copies in BALs and we confirmed similar levels of HMPV-N gene copies in animals infected with rHMPV, Metavac® or Metavac®-RSV viruses i.e. 2.5×10^5, 4.2×10^4 or 1.1×10^5 respectively (**Figure 4B**). As expected, the RSV-F gene was detected only in animals infected with Metavac®-RSV (**Figure 4C**).

At 5 dpi, mice were euthanized to investigate inflammatory profile by histopathological scoring of lung compartments. In agreement with the weight curves, mean cumulative histopathological scores were significantly lower after infection with either Metavac® or Metavac®-RSV, compared to the rHMPV group (the scores of 4 and 4 *versus* 10, respectively), particularly owing to the absence of pleura inflammation and reduction in peribronchial, perivascular and interstitial inflammation (**Figure 4D**). We then extracted total RNA from fixed paraffin-embedded lung tissues to estimate viral load by RT-qPCR at 5 dpi. We quantified a mean number of 2.61×10^2, 8.7×10^1 or 1.1×10^2 of HMPV-N gene copies in lungs of mice infected with either rHMPV, Metavac® or Metavac®-RSV, respectively (**Figure 4E**). In agreement with the viral detection in BALs at 2 dpi, we also detected a mean number of 1.4×10^2 of RSV-F gene copies in mice infected with Metavac®-RSV virus (**Figure 4F**).

Altogether, we validated that the Metavac®-RSV LAV candidate replicates in the pulmonary airways of infected mice after intranasal instillation, and induces attenuated pathology, characterized by the absence of weight loss and reduced inflammatory profile, similarly to the monovalent Metavac® LAV candidate.

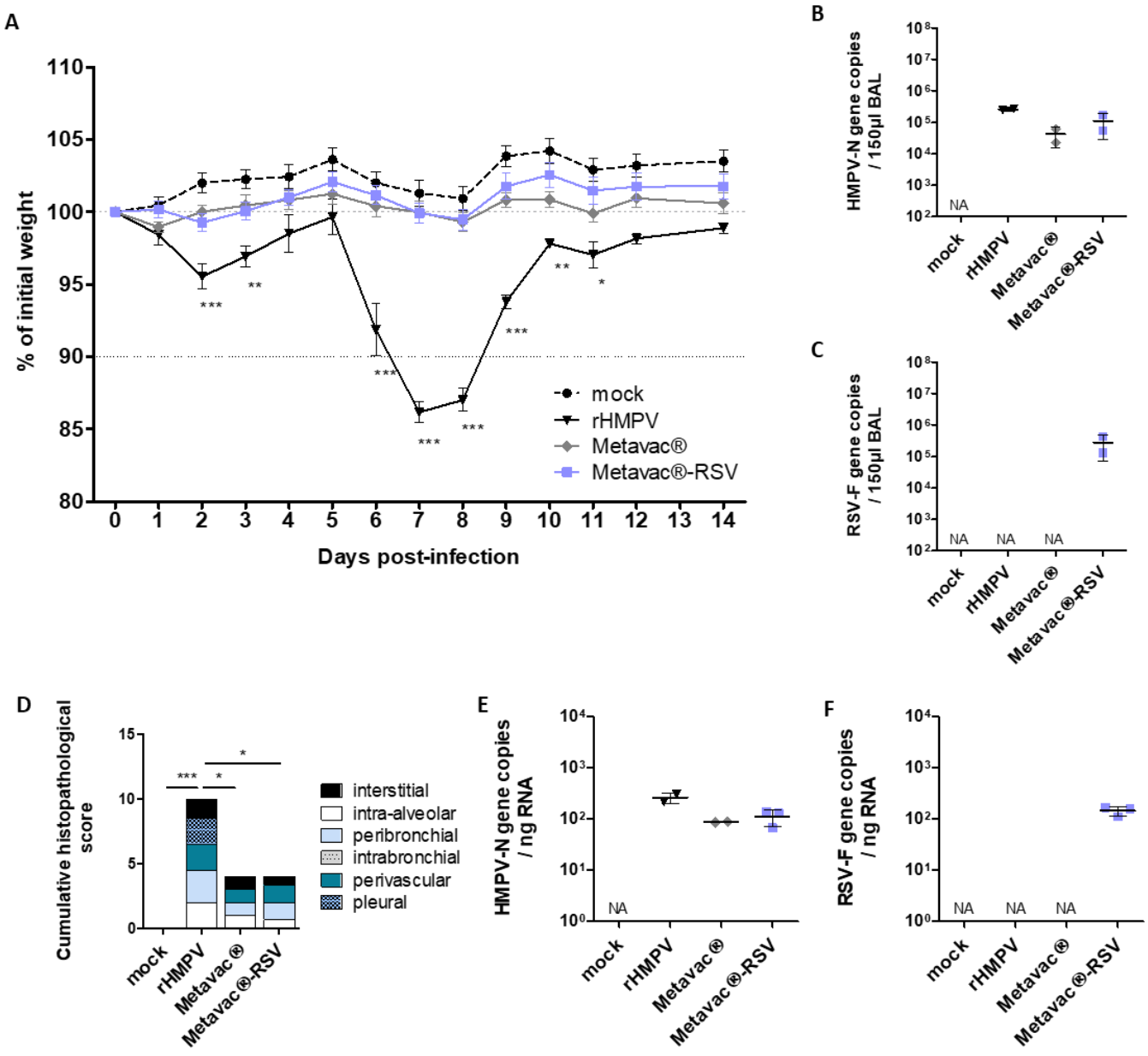

Figure 4. Viral growth and attenuation of the Metavac®-RSV vaccine candidate in BALB/c mice. BALB/c mice were infected by the IN route with 5x10^5 TCID50 of rHMPV virus, Metavac® or Metavac®-RSV vaccine candidates. (**A**) Weight loss was monitored for 14 dpi (n = 16). Data are shown as means ± SEM. *, $p < 0.05$, **, $p < 0.01$, ***, $p < 0.001$ when comparing to mock-infected mice using Repeated Measures Two-way ANOVA. (**B-C**) At 2 dpi, mice were euthanized and BAsL were harvested to measure HMPV-N gene (**B**) or RSV-F gene (**C**) copies by RT-qPCR (n = 2). (**D**) At 5 dpi, mean cumulative histopathological scores (peribronchial, intrabronchial, perivascular, interstitial, pleural and intra-alveolar inflammation scores) of the lungs from infected mice were evaluated (n = 3). *, $p < 0.05$, ***, $p < 0.001$ when comparing mean global histopathological score to mock-infected mice using One-way ANOVA. (**E-F**) At 5 dpi, HMPV-N (**E**) or RSV-F (**F**) gene copies were measured by RT-qPCR from total RNA extracted from fixed lung tissues (n=2-3). Data of viral gene quantification are shown as means ± SD.

Bivalent Metavac®-RSV vaccine candidate protects mice against lethal challenge with HMPV

We then sought to first characterize the immunogenicity and protection conferred by the Metavac®-RSV bivalent LAV candidate against HMPV viral challenges in the mouse model. BALB/c mice were immunized twice at a 21-day interval by the IN route with $5x10^5$ TCID50 of Metavac® or Metavac®-RSV vaccine candidate, or by the IM route with inactivated split HMPV adjuvanted with AddaVax™ before viral challenge with a lethal dose of rHMPV virus three weeks after the last immunization, as previously described [50]. Upon viral challenge with 2×10^6 TCID50 of rHMPV virus, mock-immunized mice showed a 100% HMPV-associated mortality at 6 post-challenge (dpc), as expected (**Figure 5A-B**). On the other hand, all three vaccinated groups showed complete protection from rHMPV-associated mortality (**Figure 5B**) and weight loss, with a maximum loss of 10,7%, 12,2% and 14.2% at 2 or 3 dpc when vaccinated with Metavac®-RSV, Metavac® or HMPV split, respectively (**Figure 5A**). In line with these results, we detected low levels of viral gene copies from nasal washes (NW) and BALs in any of the three different immunized groups at 2 dpc, in contrast to 100-fold more viral gene copies in the mock-vaccinated group (**Figure 5C**). Moreover, lung viral titers were reduced by 4 or 5 log10 in animals vaccinated with Metavac®-RSV or Metavac® LAV candidates at 5 dpc, respectively, compared to mock-vaccinated animals (**Figure 5D**). In contrast, animals vaccinated with split HMPV showed a reduction in lung viral titers of only 100-fold compared to mock, suggesting that Metavac®-RSV and Metavac® LAV candidates administrated by the IN route are more efficient in inhibiting viral replication in the lower respiratory tract (**Figure 5D**). We also confirmed that no RSV-F gene copies were detected in these tissues, showing that replicative Metavac®-RSV used for the vaccination was eliminated from the lungs at the time of the viral challenge (data not shown).

Figure 5. Efficacy of Metavac®-RSV vaccine candidate against lethal challenge with HMPV. BALB/c mice were immunized twice at a 21-day interval by the IN route with $5x10^5$ TCID50 of Metavac® or Metavac®-RSV LAV candidates or by the IM route with HMPV split preparation adjuvanted with AddaVax™. Three weeks after the last immunization, animals (n = 12/group) were inoculated with a lethal dose of rHMPV virus. (**A**) Weight loss and (**B**) mortality rates were monitored for 14 days post-challenge (dpc, n = 8/group). Data are shown as means ± SEM. ***, $p < 0.001$ when comparing to Metavac® vaccinated mice using Two-way ANOVA. (**C**) At 2 dpc, mice were euthanized and nasal washes (NW) and bronchoalveolar lavages (BAL) were harvested to measure HMPV-N gene copies by RT-qPCR (n = 2/group). (**D**) At 5 dpc, RT-qPCR was performed on total RNA recovered from mouse lung homogenates (n = 4/group) to quantify HMPV-N gene copies. (**E**) At 5 dpc, cumulative pulmonary histopathological scores (peribronchial, intrabronchial, perivascular, interstitial, pleural and intra-alveolar inflammation scores) were also evaluated (n = 3/group). Data are shown as means ± SD. *, $p < 0.05$, **, $p < 0.01$, ***, $p < 0.001$ when comparing mean global histopathological score to mock vaccinated mice using One-way ANOVA.

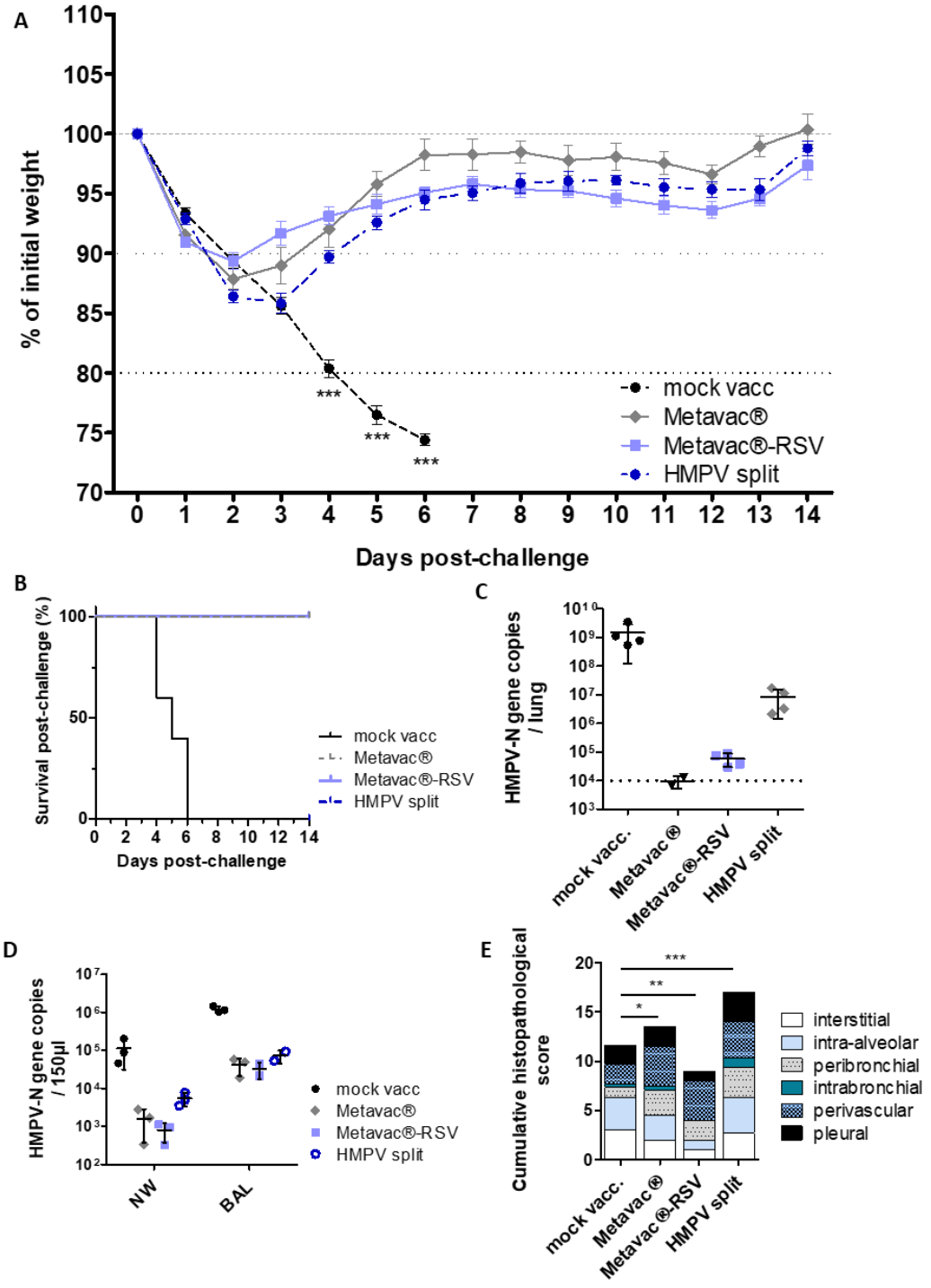

Figure 5. Efficacy of Metavac®-RSV vaccine candidate against lethal challenge with HMPV

After viral challenge, non-immunized mice developed an interstitial pneumonia of moderate intensity with a minimal-to-mild peri-bronchial and perivascular inflammation with pulmonary edema, corresponding to a mean total histopathological score of 11.66 (**Figure 5E and supplementary 1**). In comparison, the group of animals vaccinated with Metavac®-RSV virus had a reduced total inflammatory score of 9 with a significantly milder inflammation in the interstitial compartment. Animals vaccinated with Metavac® showed a mean histopathological score of 13.5 owing to peribronchial and perivascular inflammation, while interstitial pathology was slightly reduced in this group, when compared to the non-vaccinated mice. In contrast, animals vaccinated with the split HMPV showed the highest total histopathological score (mean score of 17) with moderate-to-marked changes in all the compartments, as well as eosinophil, lymphocyte, and macrophage infiltration around bronchi, in alveoli and around the blood vessels (**Figure 5E and supplementary 1)**. Overall, after infectious challenge, Metavac® and Metavac®-RSV-vaccinated animals showed signs of pulmonary inflammation, although not associated with interstitial pneumonia or exaggerated reaction, as induced by the IM administration of HMPV split.

We then investigated the levels of circulating neutralizing antibodies (NAb) and IgG (**Figure 6**) against HMPV A for the different vaccines compared to mock-vaccinated animals. Immunization with Metavac®-RSV was associated with a progressive increase in NAb levels along the protocol, reaching the highest titers at 21 dpc, similar to the Metavac®-vaccinated group (**Figure 6A**). As expected, we detected significant levels of anti-HMPV specific IgG, corresponding to the kinetics of NAb (**Figure 6D**). Interestingly, Metavac®-RSV vaccinated animals also showed the production of NAb against an heterologous HMPV B strain and RSV A virus (**Figure 6B and C**), demonstrating its ability to induce a broad immune response in vaccinated animals.

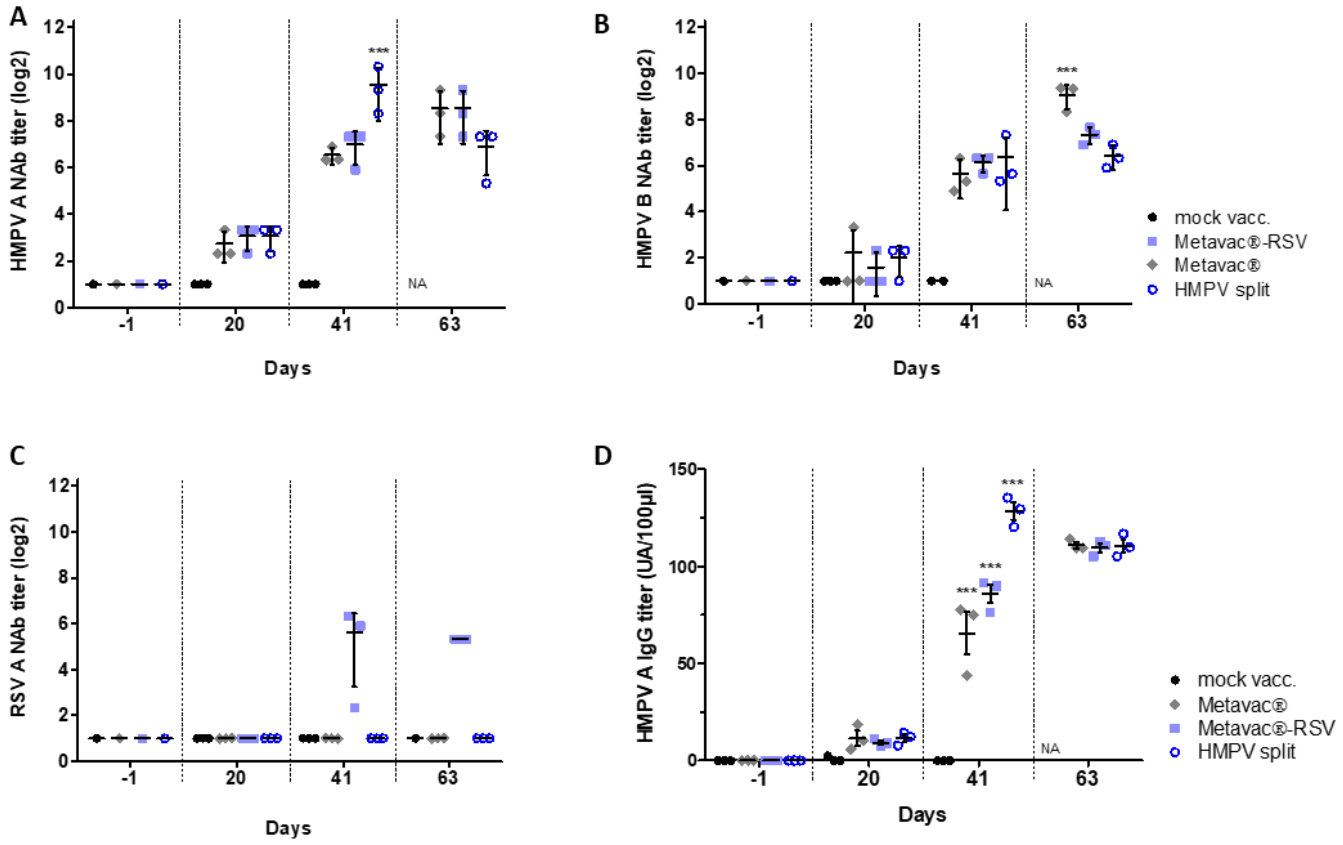

316

317

Figure 6. Immunogenicity of Metavac®-RSV vaccine candidate before and after lethal challenge with HMPV. BALB/c mice were immunized twice at a 21-day interval by the IN route with $5x10^5$ TCID50 of Metavac® or Metavac® -RSV vaccine candidates or by the IM route with the adjuvanted HMPV split preparation. Three weeks after the last immunization, animals (n = 12/group) were inoculated with a lethal dose of rHMPV. Immunogenicity of vaccine candidates was measured at -1, 20, 41 or 63 days after the first immunization by microneutralization (**A**-**B**-**C**) or ELISA (**D**) assays from pools of sera (n = 3 pools/group). Neutralization titers were defined by an endpoint dilution assay based on fluorescent detection of (**A**) HMPV A, (**B**) HMPV B or (**C**) RSV A and represented as mean log2 reciprocal neutralizing antibody (NAb) titers. (**D**) IgG titer specific to HMPV A virus was represented as arbitrary unit based on end-point absorbance. Naïve status of mice was confirmed by processing of the samples harvested one day before vaccination. Data are shown as means ± SD. *** $p < 0.001$ when comparing each vaccinated group to the mock vaccinated condition using Two-way ANOVA.

328

329

Bivalent Metavac®-RSV vaccine candidate protects mice against challenge with RSV

Finally, we analogously sought to characterize the immunogenicity and protection conferred by the Metavac®-RSV bivalent LAV candidate against RSV viral challenge in mice. We immunized BALB/c mice twice at 21-day interval by the IN route with $5x10^5$ TCID50 of Metavac-RSV vaccine candidate and then challenged mice with rRSV-Luc virus in order to compare the efficacy of the Metavac®-RSV LAV candidate to groups of mock-vaccinated mice or those vaccinated with RSV WT virus, using rRSV-mCh as a surrogate. As expected for RSV infection in the BALB/c mouse model, challenge with $1×10^5$ PFU of rRSV-Luc did not induce weight loss in mock-immunized mice, but the replication of the rRSV-Luc was followed with luciferase expression and *in vivo* imagery system. The images taken at 3 or 5 dpc showed a progressive intensification in the *in vivo* bioluminescence activity, representing increased viral replication in the lung tissue, and a constant viral replication in the nasal compartment of mock-vaccinated mice. The bioluminescence measured in mice vaccinated with Metavac®-RSV LAV candidate or RSV WT was significantly reduced in the upper and lower respiratory tracts **(Figure 7A)**, with $1.25 \times 10^5 \pm 15\ 700$, and $1.10 \times 10^5 \pm 8\ 400$ photons per second, respectively, in comparison to $4.6 \times 10^6 \pm 2.9 \times 10^6$ photons per second for mice in the mock-vaccinated group **(Figure 7B**). On 4 dpc, mice were euthanized and viral lung titers were measured by RT-qPCR. In these samples, we observed mean lung viral titer reductions of 10-fold and 1000-fold in animals vaccinated with Metavac®-RSV or RSV WT viruses, respectively, compared to mock-vaccinated animals (**Figure 7C**). As previously, we validated that no residual HMPV-N gene copies were detected after RSV challenge in Metavac®-RSV vaccinated animals (**Figure 7D**).

Lastly, we measured the level of circulating NAb and IgG against RSV in samples from vaccinated mice (**Figure 7E and F**). In comparison to the mock-vaccinated animals, the animals vaccinated with Metavac®-RSV LAV candidate developed high NAb titers after viral challenge, similar to those observed in the group vaccinated with RSV WT (**Figure 7E**). As previously observed with anti-HMPV IgG induction, we measured significant levels of anti-RSV specific IgG, following NAb kinetics along the timeline (**Figure 7F**). Interestingly, we could also measure NAb directed against a heterologous RSV strain B in animals vaccinated with Metavac®-RSV and RSV WT virus after challenge (**supplementary 2**).

Hereby, we demonstrated that the Metavac®-RSV LAV candidate administrated by the IN route is efficiently protecting vaccinated mice against both HMPV and RSV challenges, restraining viral replication in pulmonary tract of the animals and inducing a broad immune response, characterized by high titers of circulating NAb and specific IgG against both HMPV and RSV.

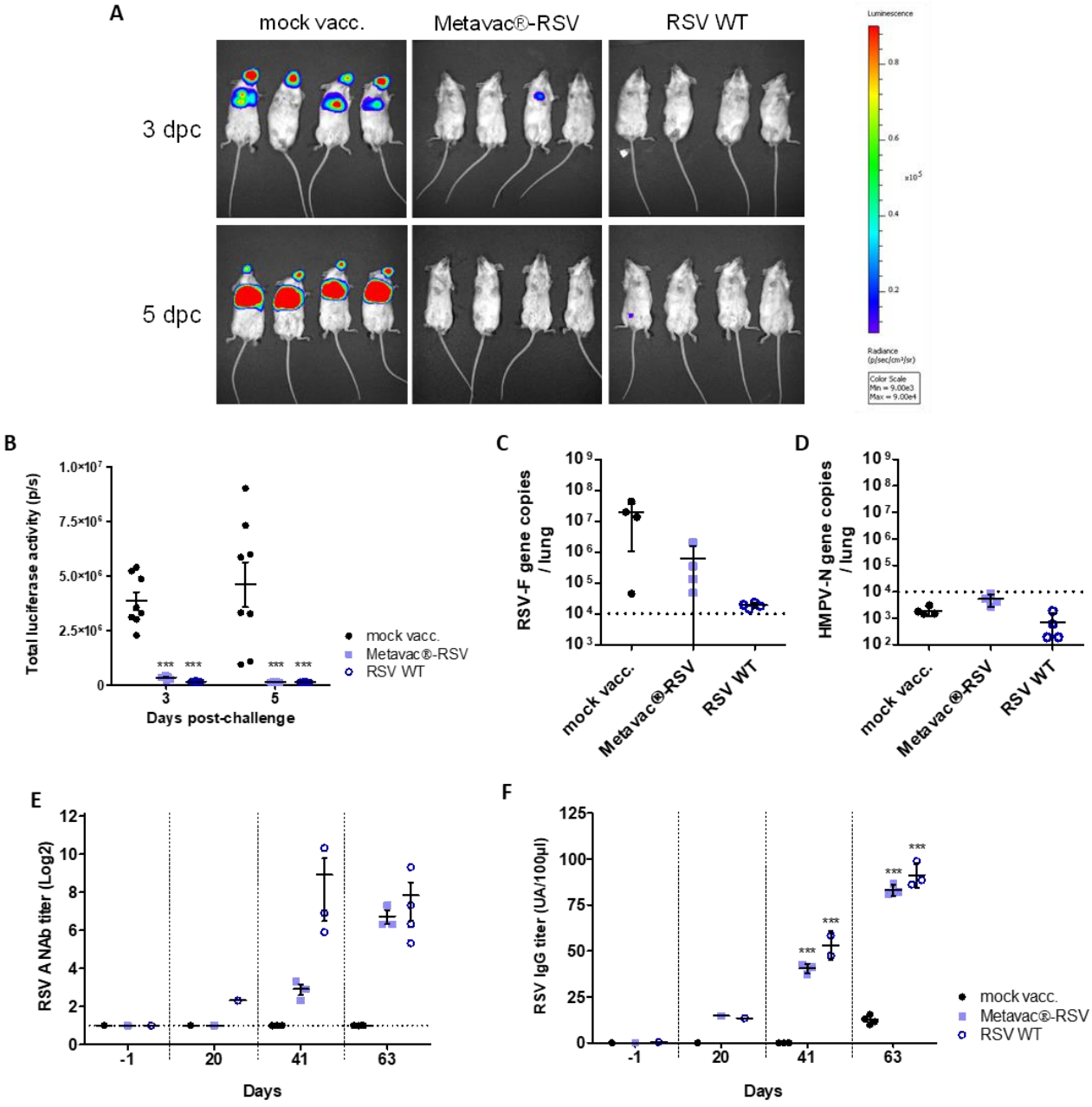

Figure 7. Efficacy and immunogenicity of Metavac®-RSV vaccine candidate following RSV challenge. BALB/c mice were immunized twice at a 21-day interval by the IN route with 5x10^5 TCID50 of Metavac®-RSV vaccine candidate or rRSV-mCh (RSV WT) virus. Three weeks after the last immunization, animals (n = 12/group) were inoculated with 1×10^5 PFU of rRSV-Luc virus. (**A-B**) Bioluminescence was measured at 3 and 5 dpc by IN injection of 50 µl of D-Luciferin (200 mM). (**A**) Ventral views of 4 representative mice were taken using the IVIS system. The scale on the right indicates the average radiance (a sum of the photons per second from each pixel inside the region of interest, ps-1 cm-2 sr-1). (**B**) Luciferase activities were quantified using 'Living Image' software and were represented as mean ± SEM photons per second (p/s) (n = 8/group). (**C-D**) RT-qPCR was performed on total RNA recovered from mouse lung homogenates (n = 4/group) harvested at 4 dpc to quantify RSV-F (**C**) or residual HMPV-N gene copies (**D**). Data are shown as means ± SD. (**E-F**) Immunogenicity of the Metavac®-RSV LAV candidate was measured before each IN instillation (-1, 20 and 41 dpi) and at the end-point (63 dpi) by RSV A microneutralization or anti-RSV IgG ELISA assays from pools of sera. (**E**) Neutralization of RSV A strain was represented as mean log2 reciprocal NAb titer. (**F**) IgG titer specific to RSV virus was represented as arbitrary unit based on end-point absorbance. *** $p < 0.001$ when comparing Metavac®-RSV or RSV WT vaccinated group to the mock vaccinated condition using Two-way ANOVA.

DISCUSSION

Despite over 60 years of research in the field of anti-RSV vaccine, a very limited number of vaccine candidates has moved to clinical phases in humans [13]. Subunit, mRNA and vectored vaccine candidates are currently the most advanced strategies for maternal or elderly vaccination. On May 2023, the GSK's vaccine (Arexvy®), a recombinant stabilized pre-fusion F protein combined to the ASO1 adjuvant, was the first vaccine approved by FDA to prevent severe RSV disease in elderly population [31]. In contrast, the development of paediatric vaccines is still ongoing; among them, there are several LAV candidates, which could induce local mucosal response through their administration by the IN route, in addition to strong T cell responses. At the same time, the development of anti-HMPV vaccines still lags behind despite the high prevalence of this viral infection in infants.

We previously presented and described Metavac®, a LAV candidate against HMPV, demonstrating strong immunogenicity, protective properties against lethal HMPV challenge in mice, and production scalability for manufacturing purposes [50,51]. Moreover, as the HMPV genome has previously been described for its property to express additional genes of interest (GFP, luciferase or additional copies of its own genes) [50,54,57–59], we hypothesized that Metavac® could offer such an advantageous property, as a versatile LAV platform capable of expressing an exogenous RSV-F protein in order to achieve broad protection against human pneumoviruses. To date, several different viruses, mainly belonging to the *Paramyxoviridae* family, have been engineered to express surface glycoproteins of RSV or HMPV [60]; however, the use of pneumoviruses as a vector has rarely been described.

In this study, we demonstrated that the addition of a supplementary RSV/A2-F coding gene within the Metavac® genome, between the endogenous F and M2 genes, resulted in efficient rescue of the chimeric Metavac®-RSV virus and subsequent incorporation of RSV-F fusion protein into viral particles, despite a significant increase of Metavac® genome length (**Figure 1**). The size of the inserted exogenous cassette could have an impact on the replication of the chimeric virus, as previously described for recombinant human parainfluenza type 3 virus (PIV3) [61], although the limit of exogenous gene incorporation into the Metavac® genome has not been determined yet. Interestingly, we noticed that the position of the RSV-F insertion was critical for rescue and replication of the recombinant virus. For example, other insertion sites, such as the 3'-proximal positions in the Metavac® genome, resulted in poorly-replicating or non-replicating viruses (data not shown), in contrary to Biacchesi and al. [58]. This discrepancy could be likely caused by the intrinsic property of the HMPV A1/C-85473 strain from which Metavac® was generated, and/or a related unbalanced expression of downstream-localised genes, resulting in the impairment of the Metavac® replicative cycle, as it was described for rB/HPIV3 [62,63] or with virus harbouring highly fusogenic phenotype [62] like that of Metavac® virus.

We reported that Metavac®-RSV replicates efficiently in LLC-MK2 cells over a 7-day period, with similar levels to those obtained with Metavac®, while displaying delayed replication kinetics (**Figure 1**). Moreover, we observed that Metavac®-RSV induced formation of large multinucleated cells (**Figure 2**), thus confirming a conserved hyperfusogenic property of its endogenous F protein, according to previous studies with the viral C-85473 background [53,54].

We then investigated RSV-F expression by immunofluorescent staining at 48 h post-infection and we observed that half of the LLC-MK2 cells infected by Metavac®-RSV expressed both RSV-F and HMPV-F proteins at their surface

(**Figure 2A**). This observation is coherent with the delayed onset of Metavac®-RSV replication kinetics (**Figure 1**). Foreseen excision of the GFP gene to reduce Metavac®-RSV genome length and longer expression kinetics studies would be useful to verify if the delay in the onset of replication is associated with the increase in the genome length. In a complementary way, co-localization of RSV and HMPV-F proteins, as revealed by co-immunostaining, might also lead to steric shielding of some epitopes and prevention of their recognition by antibodies and/or expression of hypothetical heterologous fusion protein. Although not intrinsic to all hyperfusogenic proteins, their surface expression is sometimes associated with decreased trafficking of the antigen on the surface, as demonstrated for HMPV and some mutants of Measles virus [54,64].

In the HAE model (**Figure 3**) as well as in LLC-MK2 cells (**Figure 1**), Metavac®-RSV harbored attenuated replicative properties, in comparison to its monovalent Metavac® counterpart. This could be explained by attenuating effect of the additional gene expression, a phenomenon frequently described in vectored vaccines [60]. Putative increasing fusogenic activity of the Metavac®-RSV virus due to the RSV-F protein expression must be also considered and further investigated [65]. Most importantly, the bivalent candidate was characterized as efficiently infectious and replicative in such a human differentiated airway epithelial tissue, as expected for a LAV candidate. Notably, the bivalent Metavac®-RSV expressed both RSV-F and HMPV-N proteins into the cilia at the apical surface of HAE (**Figure 3D**), where new virions bud from the cell membrane [66–68], and also where resident macrophages initiate immune responses [69–71] and where secreted IgA (sIgA), the main humoral effector, is expressed [72–74].

In line with *in vitro* results, we reported that Metavac®-RSV also replicated efficiently *in vivo*, similar to the Metavac® candidate in BALB/c mice (**Figure 4**). Importantly, the bivalent virus replicates in the respiratory tract of infected BALB/c mice as efficiently as the rHMPV, but without virus-associated weight loss, and with reduced lung inflammation and histopathology damage (**Figure 4**), as expected for LAV candidates.

Following a double vaccination regimen (prime and boost vaccination by the IN route) with Metavac®-RSV, mice were protected from subsequent rRSV-Luc challenge with a significant reduction of luciferase activity in the upper and lower respiratory tracts of challenged mice, compared to mock-vaccinated animals, and a 10-fold reduction in pulmonary viral titers as measured by RT-qPCR (**Figure 7**). Moreover, similar to previous results with the monovalent Metavac®, we demonstrated that mice vaccinated with the bivalent Metavac®-RSV were also completely protected against a lethal HMPV challenge, resulting in a 4-5 log10 decrease in pulmonary viral titers compared to mock-vaccinated animals (**Figure 5**). In line with these results, a broad antibody response (NAbs and IgGs) against both RSV and HMPV was detected in sera 20 days after the second immunization with Metavac®-RSV LAV candidate, with a further increase after virus challenge (**Figure 5**). Importantly, we also measured the induction of NAbs against heterologous RSV or HMPV strains (**Figure 6** and Supplementary), emphasizing the potential of the bivalent Metavac®-RSV LAV candidate to confer a large protection against several RSV and HMPV strains from the two major groups (A and B).

Additionally, and similar to the monovalent Metavac®, Metavac®-RSV vaccination was not associated with high immunopathology score and/or an exacerbated immune response in lungs of challenged mice, in contrast to the group vaccinated by the IM route with the split inactivated HMPV vaccine, suggesting a lower risk for Metavac® and Metavac®-RSV to predispose to enhanced pulmonary disease.

To our knowledge, our study describes, for the first time, a bivalent HMPV-based LAV candidate that replicates *in vitro* and *in vivo*, harbours an attenuated phenotype and induces homologous and heterologous neutralizing antibody responses that contribute to the efficient protection against both RSV and HMPV challenges. Further investigations in complementary (cotton rat) and more relevant preclinical (non-human primate) models must be conducted to confirm our results and to identify efficient dose vaccination strategies. Importantly, the mucosal secretory responses to Metavac®-RSV vaccination in the upper airway epithelium should be characterised, since it has been described that the role of mucosal immunity in controlling respiratory infections was major compared to that of systemic immunity [72,73,75]. Nasal secretory IgAs, which are more cross-protective than other immunoglobulins and initiate antibody-dependent cell-mediated cytotoxicity [76,77], should be particularly investigated in non-human primate models, as they seem to be the best correlate of protection in challenge studies with RSV [73] and other respiratory viruses [78,79].

Development of new vaccines against respiratory mucosal viruses remains a striking challenge, despite strong efforts in this field that resulted in the recent FDA approval of GSK's RSV-F recombinant subunit vaccine for prevention of severe RSV disease in the elderly population [31,80]. Of note, this vaccine is based on the IM delivery of recombinant pre-fusion metastable RSV-F protein that is exposing more immunogenic epitopes than the post-fusion form [81–87]. It would be interesting to associate such a conformation of RSV-F with our Metavac® LAV platform which expresses antigens at surface of virions and infected cell membranes. In this study, we demonstrated that Metavac® can be used as a versatile LAV platform for heterologous respiratory viral antigen expression. By co-expressing RSV-F and HMPV-F antigens, Metavac®-RSV constitutes an advantageous vaccine candidate, which could confer extended protection against the two prevalent respiratory pneumoviruses RSV and HMPV, responsible for the vast majority of bronchiolitis and pneumonia in infants and in the elderly. Associated to a scalable production process for manufacturing, the bivalent Metavac®-RSV LAV candidate could be a new promising option to protect children, at-risk young adults and the elderly populations that need appropriate specific strategies in term of vaccine response, schedule and regimen [88].

Acknowledgment

This study was supported by grants from Agence National de la Recherche (ANR AAP19 METAVAC-T17), and from Région Auvergne-Rhône-Alpes (R&D booster METABIOSE, Installations de Recherche et d'Innovation Centrées Entreprises, IRICE, and Pack Ambition International 2021, LIA RespiVir) to Manuel Rosa-Calatrava and a grant from Canadian Institutes of Health Research (No. 148361) to Guy Boivin. Caroline Chupin received the support of the Association Nationale Recherche Technologie (ANRT).

The authors would like to thank Dr. Marie-Anne Rameix-Welti for the construction of recombinant rRSV-GFP virus and the Centre d'Imagerie Quantitative Lyon-Est (CIQLE) for support at the EM, confocal and histology platforms. For access to animal experiment facilities, the authors thank the Infectiology of fishes and rodent facility (IERP, INRAE, ref)) and the CELPHEDIA Infrastructure (http://www.celphedia.eu/), especially the center AniRA PBES facility in Lyon. The authors acknowledge the contribution of the Emerg'in platform for access to IVIS200 that was financed by the Region Ile De France (SESAME).

Author contribution

Conceptualization: D.O-M, J-F.E., J.D., G.B., M.R-C.

Methodology: D.O-M, J.D., J.C., S.P., O.T.

Validation: J.D., G.B., M.R-C.

Formal analysis: D.O-M, J.D., J.C., M-E.H.

Investigation: D.O-M, A.T, P.B, C.C, C.D, V.D, E.L, A.P, M.G, J.D., C.V.

Resources: G.B., M.R-C., M-E.H.,

Data curation: J.D

Writing—original draft preparation: D.O-M, J.D., M.R-C.

Writing—review and editing: D.O-M, J.D., J-F.E., M-E.H., S.P, G.B., M.R-C.

Visualization: D.O-M, J.D.

Supervision: J.D., M-E.H., G.B., M.R-C.

Project administration: D.O-M, J.D., G.B., M.R-C.

Funding acquisition: G.B., M.R-C.

Declaration of interests

Manuel Rosa-Calatrava, Guy Boivin, Julia Dubois and Marie-Eve Hamelin are co-founders and shareholders of Vaxxel SAS. Andrés Pizzorno and Olivier Terrier are shareholders of Vaxxel SAS. Julia Dubois was R&D project manager of Vaxxel SAS. Caroline Chupin is employee of Vaxxel SAS. The other authors declare no competing interests.

The authors declare the following patent : EP22305240.2 – PCT/EP2023/055221 concerning Vaccine composition against two respiratory viruses (Inventors: Daniela Ogonczyk-Makowska, Jean-François Eléouët, Guy Boivin, Julia Dubois and Manuel Rosa-Calatrava ; Applicants : Institut National de la Santé et de la Recherche Médicale (INSERM), Centre National de la Recherche Scientifique (CNRS), Université Claude Bernard Lyon 1 (UCBL) Ecole Normale Supérieure de Lyon (ENS Lyon), Institut National de Recherche pour l'Agriculture, l'Alimentation et l'Environnement (INRAE) and Vaxxel SAS).

Ethics and Biosecurity

HMPV animal studies were approved by the SFR Biosciences Ethics Committee (CECCAPP C015 Rhône-Alpes, protocol ENS_2017_019) according to European ethical guidelines 2010/63/UE on animal experimentation. The protocol of RSV challenge was approved by the Animal Care and Use Committee at "Centre de Recherche de Jouy-en-Josas" (COMETHEA) under relevant institutional authorization ("Ministère de l'éducation nationale, de l'enseignement supérieur et de la recherché"), under authorization number 2015060414241349_v1 (APAFiS#600). All experimental procedures were performed in a Biosafety level 2 facility.

FIGURE LEGENDS

Figure 1. Rescue and characterization of recombinant Metavac®-RSV virus.
(A) Schematic genomic organization of the recombinant HMPV strain (rC-85473-GFP, rHMPV), monovalent Metavac® (ΔSH-rC-85473-GFP) and bivalent Metavac®-RSV (ΔSH-rC-85473-GFP/RSV-F) viruses is represented and the insertion site of the RSV-F ORF between HMPV-F and M2 genes in Metavac®-RSV genome is detailed. GS - Gene Start, GE - Gene End, IG - intergenic sequence. Sequences added to ΔSH-rC-85473-GFP genome are underlined. Genomic sequence is presented from 3′ to 5′ extremity. (**B)** After viral rescue, *in vitro* expression of the RSV-F protein at the surface of Metavac®-RSV viral particles was visualized by transmission electron microscopy after immunogold labelling with anti-HMPV serum (5 nm bead) and the Palivizumab (15 nm bead, black arrowhead) Scale bar = 100nm. (**C)** Viral replication kinetics of the Metavac®-RSV virus were measured in LLC-MK2 cells and compared to the monovalent Metavac® counterpart. Over a 7-day period, culture supernatants were harvested and titrated in TCID50/ml. Results represent the mean of 3 experimental replicates for each time-point. * $p< 0.05$, ** $p < 0.01$, *** $p < 0.001$ when comparing Metavac®-RSV to Metavac® virus using repeated measures two-way ANOVA.

Figure 2. Co-immunostaining of HMPV and RSV-F glycoproteins in infected LLC-MK2 cells.
(A) LLC-MK2 cells were infected with GFP-expressing Metavac®, Metavac®-RSV or RSV (rRSV-GFP) viruses, fixed and stained at 3 dpi with Palivizumab (red), HMPV24 mAb (white) and DAPI (blue). Merged fluorescent signals are represented (yellow). Images of representative cytopathic effects (CPEs) were taken using Zeiss880 confocal microscope (40x magnification) and processed with ImageJ software. A numeric focus was made on CPEs (square) and presented in the right panel. (**B)** LLC-MK2 cells were infected with MOI 0.5 of either Metavac® (a-e) or Metavac®-RSV (f-j), and antigens expression on the surface of the infected cells was measured by flow cytometry 48h post-infection. HMPV-F protein was detected with HMPV24 mAb conjugated with Alexa Fluor™ 647 and RSV-F protein was detected with Palivizumab conjugated with R-Phycoerythrin. Cells were sorted and analyzed by LSR II Flow Cytometer (BD biosciences®). Approximately 30,000 single live cells were counted per each sample performed in triplicate. The figure shows representative gating of sub-populations on one of the three samples. (a,f) - all cells in the sample; (b,g) – single cells (c,h) – single live cells (d,i) – single live cells positive or negative for GFP expression (e, j) - the percentage of GFP-expressing infected single live cells with HMPV-F expression revealed by HMPV24 mAb and RSV-F expression revealed by Palivizumab.

Figure 3. Viral replication and RSV-F expression in human airway epithelium (HAE) model. Reconstituted HAE were infected with Metavac® or Metavac®-RSV viruses at an MOI of 0.1 and monitored for 7 days. (**A**) Viral spread in HAE was monitored at 3, 5 and 7 dpi by GFP fluorescence observation (10× magnification). (**B-C**) Viral quantification from epithelium apical washes collected after 1, 3, 5 and 7 dpi was performed byRT-qPCR targeting the HMPV-N gene (**B**) or the RSV-F gene (**C**). Data are shown as means ± SD and represent experimental triplicates. Dotted line represents the RT-qPCR quantification threshold. ** $p < 0.01$ when comparing Metavac®-RSV to Metavac® virus using repeated measures two-way ANOVA. (**D**) Co-immunostaining of HMPV-N and RSV-F proteins was realized at 3 dpi. Fixed HAE infected by Metavac®, Metavac®-RSV or rRSV-GFP viruses were stained with mixture of mAbs specific to the HMPV-N protein (mAb hMPV123, green), RSV-F protein (Palivizumab, red) and with DAPI (blue) specific to the nucleus. Acquisition of images of representative infected area was performed with confocal inverted microscope (Zeiss Confocal LSM 880) and processed with ImageJ software. Scale bar = 20μm. A focus on apical surface of ciliated infected cells was made (square) and is presented in the right panel.

Figure 4. Viral growth and attenuation of the Metavac®-RSV vaccine candidate in BALB/c mice. BALB/c mice were infected by the IN route with $5x10^5$ TCID50 of rHMPV virus, Metavac® or Metavac®-RSV vaccine candidates. (**A**) Weight loss was monitored for 14 dpi (n = 16). Data are shown as means ± SEM. *, $p < 0.05$, **, $p < 0.01$, ***, $p < 0.001$ when comparing to mock-infected mice using Repeated Measures Two-way ANOVA. (**B-C**) At 2 dpi, mice were euthanized and BAsL were harvested to measure HMPV-N gene (**B**) or RSV-F gene (**C**) copies by RT-qPCR (n = 2). (**D**) At 5 dpi, mean cumulative histopathological scores (peribronchial, intrabronchial, perivascular, interstitial, pleural and intra-alveolar inflammation scores) of the lungs from infected mice were evaluated (n = 3). *, $p < 0.05$, ***, $p < 0.001$ when comparing mean global histopathological score to mock-infected mice using One-way ANOVA. (**E-F**) At 5 dpi, HMPV-N (**E**) or RSV-F (**F**) gene copies were measured by RT-qPCR from total RNA extracted from fixed lung tissues (n=2-3). Data of viral gene quantification are shown as means ± SD.

Figure 5. Efficacy of Metavac®-RSV vaccine candidate against lethal challenge with HMPV. BALB/c mice were immunized twice at a 21-day interval by the IN route with $5x10^5$ TCID50 of Metavac® or Metavac®-RSV LAV candidates or by the IM route with HMPV split preparation adjuvanted with AddaVax™. Three weeks after the last immunization, animals (n = 12/group) were inoculated with a lethal dose of rHMPV virus. (**A**) Weight loss and (**B**) mortality rates were monitored for 14 days post-challenge (dpc, n = 8/group). Data are shown as means ± SEM. ***, $p < 0.001$ when comparing to Metavac® vaccinated mice using Two-way ANOVA. (**C**) At 2 dpc, mice were euthanized and nasal washes (NW) and bronchoalveolar lavages (BAL) were harvested to measure HMPV-N gene copies by RT-qPCR (n = 2/group). (**D**) At 5 dpc, RT-qPCR was performed on total RNA recovered from mouse lung homogenates (n = 4/group) to quantify HMPV-N gene copies. (**E**) At 5 dpc, cumulative pulmonary histopathological scores (peribronchial, intrabronchial, perivascular, interstitial, pleural and intra-alveolar inflammation scores) were also evaluated (n = 3/group). Data are shown as means ± SD. *, $p < 0.05$, **, $p < 0.01$, ***, $p < 0.001$ when comparing mean global histopathological score to mock vaccinated mice using One-way ANOVA.

Figure 6. Immunogenicity of Metavac®-RSV vaccine candidate before and after lethal challenge with HMPV. BALB/c mice were immunized twice at a 21-day interval by the IN route with $5x10^5$ TCID50 of Metavac® or Metavac®-RSV vaccine candidates or by the IM route with the adjuvanted HMPV split preparation. Three weeks after the last immunization, animals (n = 12/group) were inoculated with a lethal dose of rHMPV. Immunogenicity of vaccine candidates was measured at -1, 20, 41 or 63 days after the first immunization by microneutralization (**A**-**B**-**C**) or ELISA (**D**) assays from pools of sera (n = 3 pools/group). Neutralization titers were defined by an endpoint dilution assay based on fluorescent detection of (**A**) HMPV A, (**B**) HMPV B or (**C**) RSV A and represented as mean log2 reciprocal neutralizing antibody (NAb) titers. (**D**) IgG titer specific to HMPV A virus was represented as arbitrary unit based on end-point absorbance. Naïve status of mice was confirmed by processing of the samples harvested one day before vaccination. Data are shown as means ± SD. *** $p < 0.001$ when comparing each vaccinated group to the mock vaccinated condition using Two-way ANOVA.

Figure 7. Efficacy and immunogenicity of Metavac®-RSV vaccine candidate following RSV challenge. BALB/c mice were immunized twice at a 21-day interval by the IN route with $5x10^5$ TCID50 of Metavac®-RSV vaccine candidate or rRSV-mCh (RSV WT) virus. Three weeks after the last immunization, animals (n = 12/group) were inoculated with $1×10^5$ PFU of rRSV-Luc virus. (**A-B**) Bioluminescence was measured at 3 and 5 dpc by IN injection of 50 µl of D-Luciferin (200 mM). (**A**) Ventral views of 4 representative mice were taken using the IVIS system. The scale on the right indicates the average radiance (a sum of the photons per second from each pixel inside the region of interest, ps-1 cm-2 sr-1). (**B**) Luciferase activities were quantified using 'Living Image' software and were represented as mean ± SEM photons per second (p/s) (n = 8/group). (**C-D**) RT-qPCR was performed on total RNA recovered from mouse lung homogenates (n =

4/group) harvested at 4 dpc to quantify RSV-F (**C**) or residual HMPV-N gene copies (**D**). Data are shown as means ± SD. (**E-F**) Immunogenicity of the Metavac®-RSV LAV candidate was measured before each IN instillation (-1, 20 and 41 dpi) and at the end-point (63 dpi) by RSV A microneutralization or anti-RSV IgG ELISA assays from pools of sera. (**E**) Neutralization of RSV A strain was represented as mean log2 reciprocal NAb titer. (**F**) IgG titer specific to RSV virus was represented as arbitrary unit based on end-point absorbance. *** $p < 0.001$ when comparing Metavac®-RSV or RSV WT vaccinated group to the mock vaccinated condition using Two-way ANOVA.

MATERIALS AND METHODS

Cells and viruses

LLC-MK2 (ATCC CCL-7) cells were cultivated in minimal essential medium (MEM, Life Technologies) supplemented with 10% fetal bovine serum (FBS, Wisent, St. Bruno, QC, Canada), 1% penicillin/streptomycin (Pen/Strep, 10,000 U/mL, Gibco, Thermo Fisher Scientific, Waltham, MA, USA) and 2% L-glutamin (L-Glu, Gibco, Thermo Fisher Scientific, Waltham, MA, USA). HEP-2 (ATCC CCL-23) cells were cultivated in MEM medium supplemented with 5% FBS, 1% Pen/Strep and 2% L-Glu. Vero cells (ATCC CCL-81) were cultivated in MEM medium 4,5g/l glucose supplemented with 5% FBS, 1% Pen/Strep and 2% L-Glu. BHK-T7 cells (a kind gift from Dr Ursula Buchholz at the NIAID in Bethesda, MD) were maintained in MEM supplemented with 10% FBS, 1% Pen/Strep, additionally supplemented with 1% non-essential amino acids (NEAA, Life Technologies) and 0.2 mg/mL geneticin (G418, Life Technologies) added every other passage.

Recombinant HMPV viruses rC-85473-GFP (rHMPV), rCAN98-75-GFP, Metavac® (ΔSH-rC-85473-GFP) and Metavac®-RSV were rescued and produced using BHK-T7 and LLC-MK2 cells, as previously described [53]. Recombinant RSVs expressing fluorescent proteins: GFP (rRSV-GFP), mCherry (rRSV-mCh) and Luciferase (rRSV-Luc).

Molecular biology

RNA of RSV strain A2 virus was isolated from cell culture (Qiamp MiniElute Viral RNA Spin Protocol) and reverse-transcribed with Superscript II RT reverse transcriptase (Thermo Fisher Scientific, 18064014). The cDNA product was used as a matrix for amplification of RSV-F ORF using Q5 DNA polymerase (New England BioLabs, M0491L) with appropriate primers (forward: 5′- GAGTGGGACAAGTGAAAATGG-3′, reverse: 5′-GATTT-GTCCCAAATTTTTATTTTTATTTTATTTTAATTTTAATTTTATTTTATTTTAATTTAATTTACTTTATTTTTAATTAATTAGTT-3′). RSV-F gene was flanked by HMPV-derived Gene Start and Gene End signals (Figure 1A) and HMPV genome overlapping regions were added at the 5′ and 3′ extremities of the RSV-F amplicon.

The pSP72 plasmid containing the complete genome of Metavac® (pSP72-ΔSH-rC-85473-GFP/ pSP72-Metavac®) virus [50,51] was amplified with Q5 DNA polymerase using primers matching the intergenic F-M2 region (forward: 5′-AACTAATTAATTAAAAATAAAGTAAATTAAATTAAAATAAAATAAAATTAAAATTAAAA-TAAAATAAAAATAAAAATTTGGGACAAATC-3′, and reverse 5′-CCATTTTCACTTGTCCCACTC-3′).

The RSV-F amplicon was then inserted into the linearized pSP72-Metavac® vector by Gibson Assembly® Cloning Kit (New England Biolabs, E5510S) in 2-fragment cloning reaction, following provider's recommendations. Briefly, 75

ng of linearized vector with 3-fold molar excess of insert were used. The reaction product was then diluted 4 times in distilled water, and 2 µl were transformed into Stellar™ Competent Cells (Takara Bio). Bacteria were plated in selective medium containing Ampicillin and plasmids were isolated by Gene Elute Plasmid Purification Kit (Sigma-Aldrich). Complete plasmid DNA sequence was confirmed by Sanger sequencing.

Reverse genetics

BHK-T7 cells at 75% confluency were co-transfected with four supporting plasmids encoding ORFs of N, P, L and M2-1 of HMPV strain B2/CAN98-75, as well as with pSP72 plasmid containing the full-length antigenome of Metavac®-RSV virus using Lipofectamine 2000 (Thermo Fisher Scientific, Life Technologies), according to a previously described protocol [53]. Transfected cells were incubated at 37°C and 5% CO_2 for 2 days until the GFP expression was noticeable. Next LLC-MK2 cells were added for co-culture in OptiMEM infection medium supplemented with fresh 0.0002% trypsin, as previously described [53]. Cells were scraped, sonicated, centrifuged and the supernatant was diluted to inoculate newly seeded LLC-MK2 monolayers. After several cell passages, recombinant Metavac®-RSV virus was concentrated by ultracentrifugation at 28 000 rpm, resuspended in OptiMEM and stored at -80°C. Viral stocks were titrated as 50% tissue culture infectious doses (TCID50)/ml.

Immunostaining

For various immunostaining assays, we used the humanized anti-RSV-F monoclonal antibody (mAb) Palivizumab (Synagis®, AstraZeneca™), anti-HMPV-F mAb (HMPV24, Abcam ab94800), anti-HMPV-N mAb (HMPV123, Abcam ab94803), in-house polyclonal HMPV- or RSV-specific murine sera, respectively generated by mouse infection with HMPV C-85473 or RSV A2 viruses.

For flow cytometry assays, HMPV24 mAb was conjugated with fluorochrome Alexa Fluor™ 647 (Alexa Fluor 647 Antibody Labeling Kit, Invitrogen, A20186), and Palivizumab was conjugated with fluorochrome R-Phycoerythrin (PE / R-Phycoerythrin Conjugation Kit - Lightning-Link®, Abcam, ab102918).

Transmission Electron Microscopy

Metavac® and Metavac®-RSV viruses were produced in LLC-MK2 cells and concentrated by ultracentrifugation, as previously described [50]. Viral pellets were then resuspended in 0.9% NaCl and passed through 0.45 µm filter. Viral suspensions were adsorbed on 200-mesh nickel grids coated with formvar-C for 10 min at room temperature (RT). Immunogold labelling was performed the next day by flotation the grids on drops of reactive media. Nonspecific sites were coated with 1% BSA in 50 mM Tris-HCl (pH 7.4) for 10 min at RT then incubated in wet chamber with Palivizumab diluted in 1% BSA, 50 mM Tris-HCl (pH 7.4) for 2 h at RT. The grids were washed successively in 50 mM Tris-HCl (pH 7.4 and then pH 8.2), incubated with 1% BSA, 50 mM Tris-HCl (pH 8.2) for 10 min at RT, and labeled with 15 nm gold conjugated goat anti-human IgG (Aurion) diluted 1/50 in 1% BSA, 50 Mm Tris-HCl (pH 8.2) for 45 min. A second immunogold labelling with in-house anti-HMPV murine serum was then performed following the same protocol. Finally,

the immunocomplex was fixed with 2% glutaraldehyde diluted in 50 mM Tris-HCl (pH 7.4) for 2 min and grids were stained with UranyLess (Electron Microscopy Sciences, 22409) for 1 min and observed on a transmission electron microscope (Jeol 1400 JEM, Tokyo, Japan) equipped with a Gatan camera (Orius 1000) and Digital Micrograph Software.

Replication kinetics

Confluent monolayers of LLC-MK2 cells were washed with PBS and infected with a MOI of 0.01 of Metavac®-RSV or Metavac® vaccine candidates diluted in OptiMEM. Cells were incubated 1,5 h at 37°C, then infectious media was aspirated and replaced by fresh OptiMEM with 0.0002% trypsin. Infected cells were incubated at 37^{0}C and 5% CO_2 and supernatants were harvested in triplicate at daily intervals for 7 days then frozen at -80^{0}C. Each sample was thawed and used for determination of TCID50/ml in LLC-MK2 cells.

Confocal microscopy

For confocal microscopy observations, confluent monolayers of LLC-MK2 cells grown on Lab-Tek II chamber slides (ThermoFisher Scientific) were infected with a MOI of 0.01 of recombinant Metavac®, Metavac®-RSV or rRSV-GFP viruses. After 3 days of infection, infected cells were fixed with 4% paraformaldehyde in PBS for 30 min at 4°C, washed in PBS 1X, permeabilized with 0.1% Triton X-100 in PBS (PBS-T) and blocked with 1% SVF for 30 min. Then, anti-RSV-F Palivizumab and anti-HMPV-F HMPV24 antibodies were used as primary antibodies in PBS-T at 1/5000 and 1/500 dilutions, respectively. After 1 h-incubation, the cells were washed in PBS-T and then incubated with goat anti-human mAb conjugated with AlexaFluor 546 and goat anti-mouse mAb conjugated with AlexaFluor 633 (ThermoFisher Scientific) for 30 min at 1/100 dilution. Nuclei were counterstained with DNA-binding fluorochrome 4,6-diamidinon-2-phenylindole (DAPI, Invitrogen). After staining, the coverslips were mounted with Fluoromount G (Cliniscience) and analyzed using a confocal inverted microscope (Zeiss Confocal LSM 880).

Flow cytometry

For flow cytometry assays, confluent monolayers of LLC-MK2 cells grown in 24-well plates were infected with a MOI of 0.5 of Metavac®-RSV or Metavac® vaccine candidates. After 1.5 h of virus adsorption, infection medium was replaced by fresh OptiMEM with 0.0002% trypsin. At 48 h post-infection, cells were washed with cold PBS, trypsynised and resuspended in cold PBS 2% FBS. A wash with cold PBS 2% FBS was performed between each step involving antibodies. First, cells were incubated with optimized concentration of CD16/CD32 antibody (Invitrogen, 14-0161-82) and viability dye (LIVE/DEAD™ Fixable Near-IR Dead Cell Stain Kit, ThermoFisher Scientific, L34975) for 30 min at 4°C. After subsequent washes, samples were incubated for 30 min at 4°C with optimized concentration of HMPV24 mAb conjugated with Alexa Fluor 647 and Palivizumab conjugated with R-Phycoerythrin. Cells were sorted and analyzed by LSR II Flow Cytometer (BD biosciences®) cytometer to determine: the percentage of infected GFP-positive cells, the percentage of GFP-positive cells with simultaneous HMPV-F and RSV-F expression revealed by HMPV24 antibody and Palivizumab, respectively. Compensation control for the viability dye was performed with live and dead

LLC-MK2 cells. Compensation controls for conjugated antibodies were performed using compensation beads (UltraComp eBeads™ Compensation Beads, ThermoFisher Scientific, 01-2222-42). Approximately 30,000 single live cells were counted per sample, and the experiment was performed in triplicate.

Infection of reconstituted human airway epithelium

In vitro reconstituted human airway epithelium (HAE), derived from healthy donors' primary nasal cells (MucilAir™), was purchased from Epithelix (Plan-les-Ouates, Switzerland). HAEs were incubated with a MOI of 0.1 of Metavac® or Metavac®-RSV for 2 h at 37°C, 5% CO_2. Infections were monitored for 7 days post-infection (dpi). At 3, 5 and 7 dpi, apical washes with warm OptiMEM were performed in order to extract viral RNA (QIAamp Viral RNA kit, Qiagen, Hilden, Germany) and the images of infected HAEs were taken by fluorescent microscopy with EVOS M5000 Cell Imaging System (Invitrogen, ThermoFisher Scientific).

For fluorescence immunostaining, infected HAEs with a MOI of 0.1 of Metavac®, Metavac®-RSV or rRSV-GFP were rinsed three times with 1X Dulbecco's PBS (DPBS, Gibco, 14190) at 3 dpi and fixed for 50 min in 4% paraformaldehyde solution (Electron microscopy science, 15710) at RT. HAEs were rinsed three more times in DPBS, then the tissue was embedded in paraffin, and sections of 5 µm-thick slices were prepared using a microtome. Immunostaining was then performed with Discovery XT (Roche) device. Fixed tissues were first deparaffinized and incubated with RiboCC citrate buffer (pH 6.0) for 16 min. The slices were subsequently stained with primary antibodies Palivizumab and HMPV123 mAb at 1:1000 or 1:100 dilutions, respectively, for 1 h at 37°C, and then with secondary antibodies (Alexa 488 GAR Invitrogen, A11 008 or Alexa 594 GAH Invitrogen™, A11 014) at 1:500 or 1:300 dilution, respectively, for 1 h at 37°C. The nuclear staining was performed with DAPI. The images were acquired with inverted confocal microscope (Zeiss Confocal, LSM 880).

Real-time RT-PCR

The RNA was reverse-transcribed at 42°C using SuperScript™ II RT (Invitrogen) with random primers. Amplification of the HMPV-N gene was performed by RT-qPCR using Express one-step SYBR GreenER mix, premixed with ROX (ThermoFisher Scientific) and with forward primer 5'-AGAGTCTCAGTACACAATAAAAAGAGATGTGGG-3' and reverse primer 5'-CCTATTTCTGCAGCATATTTGTAATCAG-3, and amplification of the RSV-F gene was performed using forward primer 5'-CTGTGATAGARTTCCAACAAAAGAACA-3' and reverse primer 5'-AGTTACACCTGCATTAACACTAAATCC-3'. The calibration of HMPV-N and RSV-F copies was assessed by amplification of a plasmid.

Animal studies

For *in vivo* infection studies, 4-6-week-old BALB/c mice (Charles River Laboratories), randomly housed in groups of 5-6 per micro-isolator cage, were infected *via* IN route with 5×10^5 TCID50 of rHMPV, Metavac® or Metavac®-RSV under ketamine/xylazine anesthesia. As a control group, mice were mock-infected IN with OptiMEM medium. Animals

were monitored daily for 14 days for weight loss, clinical disease signs, reduced activity, or ruffled fur, and were euthanized upon 20% loss of the initial weight. Mice were euthanized using sodium pentobarbital at 2 dpi (n=2/group) to perform broncho-alveolar lavages (BAL) for viral genes quantification by RT-qPCR, or at 5 dpi (n=3/group) to harvest their lungs for histopathological analysis (NovaXia Pathology Laboratory). For histopathological analysis, lungs were perfused with 2% formaldehyde at the time of the harvest and until the paraffin embedding. Retrospectively, the quantification of viral gene expression by RT-qPCR was also performed from fixed lung slices after total RNA extraction using RNeasy® DSP FFPE Kit (Qiagen), following manufacturer instructions.

For the vaccination studies, 4-6 week-old BALB/c mice were immunized twice at a 21 day-interval before receiving a viral challenge 21 days after the last immunization. Animals were monitored daily for 14 days after each immunization or infection for weight loss, clinical signs, reduced activity or ruffled fur and were euthanized upon 20% loss of their initial weight.

To assess the protection against HMPV challenge, sixteen animals were immunized by the IN route with 5×10^5 TCID50 of Metavac® or Metavac®-RSV, or by IM route with HMPV split preparation consisting of inactivated HMPV C-85473 virus, as previously described **[89]**, diluted 1:1 with squalene-based oil-in-water nano-emulsion AddaVax™ (Invivogen). Mice mock-infected IN with OptiMEM (mock vacc.) were used as a negative control vaccination group. Twenty-one days after the second immunization, each mouse was infected with $2x10^6$ TCID50 of rHMPV, expected to induce lethality in more than 80% of the animals. At 2 days post-challenge (dpc), mice were euthanized (n = 2/group) to collect nasal washes (NW) and bronchoalveolar lavages (BAL) in PBS 1X to measure HMPV-N gene copies by RT-qPCR. Viral titers (n=4/group) and histopathological scores (n=3/group) were evaluated at 5 dpc from lung homogenates or from formaldehyde-fixed tissues, respectively, as previously described **[50]**. Prior to immunizations (day -1 or day 20), prior to challenge (day 41) and 21 days after challenge (day 63), blood samples were taken by sub-mandibular bleeding or cardiac puncture at the terminal time-point to evaluate neutralizing antibodies (NAbs) and IgG titers.

To evaluate the protection against RSV challenge, twelve animals were immunized by the IN route with 5×10^5 TCID50 of Metavac®-RSV or with 5×10^5 PFU of rRSV-mCh viruses. As a negative control group of vaccination, mice were mock-infected IN with OptiMEM (mock vacc.). Twenty-one days after the second immunization, each mouse was infected with an inoculum of 3,75 x 10^5 PFU of rRSV-Luc virus, as previously described **[90]**. To determine *in vivo* bioluminescence intensity, mice (n=8/group) were anaesthetized 3 and 5 dpc and observed alive using the IVIS imaging system 5 min after IN injection of D-luciferin. At 4 dpc, mice were euthanized (n = 4/group), lungs homogenized in 1 ml of PBS 1X before total RNA extraction and the quantification of RSV-F and HMPV-N genes by RT-qPCR was performed as previously described. Prior to immunizations (days -1 or day 20), prior to challenge (day 41) and 21 days after challenge (day 63), blood samples were taken by sub-mandibular bleeding or cardiac exsanguination at the terminal time-point to evaluate neutralizing antibody (NAb) and IgG titers.

Neutralization assays

To evaluate the production of a specific neutralizing antibody response, sera were recovered from blood samples, pooled and heat-inactivated at 56°C until testing. Serial two-fold dilutions of sera in infection medium were then tested for neutralization of homologous rHMPV (rC-85473-GFP), heterologous HMPV (rCAN98-75-GFP) or rRSV-mCh viruses on LLC-MK2 cells or Vero cells, respectively. Reciprocal neutralizing antibody titers were determined by an end-point dilution assay, based on fluorescent detection (Spark® multimode microplate reader, TECAN). Neutralization of infection was defined as more than 75% decrease in the fluorescence, compared to the negative infection control.

IgG quantification by ELISA assays

To detect HMPV- or RSV-specific IgG, NUNC Maxi-Sorp 96-well plates (ThermoFisher Scientific) were coated with inactivated virus stocks (HMPV C-85473 or RSV A2 strains, respectively) diluted in carbonate-bicarbonate buffer (0.1M, pH 9,6) to 4μg/ml concentration. Plates were subsequently blocked with 5% milk in PBS-T and incubated with serum sample diluted in 5% milk in PBS-T. Specific IgG antibodies were detected using an anti-mouse IgG-HRP mAb (SouthernBiotech, ref 1031-05). ELISAs were developed using tetramethylbenzidine (TMB SureBlue, SeraCare) and the reaction was stopped with 2N H_2SO_4. Background from empty control wells was subtracted to acquire final absorbance values at 450 nm and the results were represented as arbitrary units to compare IgG titers at an optimal serum dilution.

Statistical analysis

Statistical analyses were performed with GraphPad Prism7 using One-way or Two-way ANOVA tests.

REFERENCES

1. Lozano, R.; Naghavi, M.; Foreman, K.; Lim, S.; Shibuya, K.; Aboyans, V.; Abraham, J.; Adair, T.; Aggarwal, R.; Ahn, S.Y.; et al. Global and Regional Mortality from 235 Causes of Death for 20 Age Groups in 1990 and 2010: A Systematic Analysis for the Global Burden of Disease Study 2010. *Lancet* **2012**, *380*, 2095–2128, doi:10.1016/S0140-6736(12)61728-0.
2. Li, Y.; Wang, X.; Blau, D.M.; Caballero, M.T.; Feikin, D.R.; Gill, C.J.; Madhi, S.A.; Omer, S.B.; Simões, E.A.F.; Campbell, H.; et al. Global, Regional, and National Disease Burden Estimates of Acute Lower Respiratory Infections Due to Respiratory Syncytial Virus in Children Younger than 5 Years in 2019: A Systematic Analysis. *The Lancet* **2022**, *399*, 2047–2064, doi:10.1016/S0140-6736(22)00478-0.
3. Glezen, W.P.; Taber, L.H.; Frank, A.L.; Kasel, J.A. Risk of Primary Infection and Reinfection with Respiratory Syncytial Virus. *Am J Dis Child* **1986**, *140*, 543–546, doi:10.1001/archpedi.1986.02140200053026.
4. Falsey, A.R.; Hennessey, P.A.; Formica, M.A.; Cox, C.; Walsh, E.E. Respiratory Syncytial Virus Infection in Elderly and High-Risk Adults. *N Engl J Med* **2005**, *352*, 1749–1759, doi:10.1056/NEJMoa043951.
5. Shi, T.; Denouel, A.; Tietjen, A.K.; Campbell, I.; Moran, E.; Li, X.; Campbell, H.; Demont, C.; Nyawanda, B.O.; Chu, H.Y.; et al. Global Disease Burden Estimates of Respiratory Syncytial Virus–Associated Acute Respiratory Infection in Older Adults in 2015: A Systematic Review and Meta-Analysis. *The Journal of Infectious Diseases* **2020**, *222*, S577–S583, doi:10.1093/infdis/jiz059.
6. Busack, B.; Shorr, A.F. Going Viral—RSV as the Neglected Adult Respiratory Virus. *Pathogens* **2022**, *11*, 1324, doi:10.3390/pathogens11111324.
7. Leung, J.; Esper, F.; Weibel, C.; Kahn, J.S. Seroepidemiology of Human Metapneumovirus (HMPV) on the Basis of a Novel Enzyme-Linked Immunosorbent Assay Utilizing HMPV Fusion Protein Expressed in Recombinant Vesicular Stomatitis Virus. *J Clin Microbiol* **2005**, *43*, 1213–1219, doi:10.1128/JCM.43.3.1213-1219.2005.
8. Wang, X.; Li, Y.; Deloria-Knoll, M.; Madhi, S.A.; Cohen, C.; Ali, A.; Basnet, S.; Bassat, Q.; Brooks, W.A.; Chittaganpitch, M.; et al. Global Burden of Acute Lower Respiratory Infection Associated with Human Metapneumovirus in Children under 5 Years in 2018: A Systematic Review and Modelling Study. *Lancet Glob Health* **2021**, *9*, e33–e43, doi:10.1016/S2214-109X(20)30393-4.
9. Edwards, K.M.; Zhu, Y.; Griffin, M.R.; Weinberg, G.A.; Hall, C.B.; Szilagyi, P.G.; Staat, M.A.; Iwane, M.; Prill, M.M.; Williams, J.V. Burden of Human Metapneumovirus Infection in Young Children. *N Engl J Med* **2013**, *368*, 633–643, doi:10.1056/NEJMoa1204630.
10. Barr, R.; Green, C.A.; Sande, C.J.; Drysdale, S.B. Respiratory Syncytial Virus: Diagnosis, Prevention and Management. *Ther Adv Infect Dis* **2019**, *6*, 2049936119865798, doi:10.1177/2049936119865798.
11. Widmer, K.; Zhu, Y.; Williams, J.V.; Griffin, M.R.; Edwards, K.M.; Talbot, H.K. Rates of Hospitalizations for Respiratory Syncytial Virus, Human Metapneumovirus, and Influenza Virus in Older Adults. *The Journal of Infectious Diseases* **2012**, *206*, 56–62, doi:10.1093/infdis/jis309.
12. Falsey, A.R.; Erdman, D.; Anderson, L.J.; Walsh, E.E. Human Metapneumovirus Infections in Young and Elderly Adults. *J INFECT DIS* **2003**, *187*, 785–790, doi:10.1086/367901.
13. Mazur, N.I.; Terstappen, J.; Baral, R.; Bardají, A.; Beutels, P.; Buchholz, U.J.; Cohen, C.; Crowe, J.E.; Cutland, C.L.; Eckert, L.; et al. Respiratory Syncytial Virus Prevention within Reach: The Vaccine and Monoclonal Antibody Landscape. *Lancet Infect Dis* **2023**, *23*, e2–e21, doi:10.1016/S1473-3099(22)00291-2.
14. Mac, S.; Sumner, A.; Duchesne-Belanger, S.; Stirling, R.; Tunis, M.; Sander, B. Cost-Effectiveness of Palivizumab for Respiratory Syncytial Virus: A Systematic Review. *Pediatrics* **2019**, *143*, e20184064, doi:10.1542/peds.2018-4064.
15. Keam, S.J. Nirsevimab: First Approval. *Drugs* **2023**, *83*, 181–187, doi:10.1007/s40265-022-01829-6.

16. Elawar, F.; Oraby, A.K.; Kieser, Q.; Jensen, L.D.; Culp, T.; West, F.G.; Marchant, D.J. Pharmacological Targets and Emerging Treatments for Respiratory Syncytial Virus Bronchiolitis. *Pharmacology & Therapeutics* **2021**, *220*, 107712, doi:10.1016/j.pharmthera.2020.107712.
17. Soto, J.A.; Loaiza, R.A.; Echeverría, S.; Ramírez, R.; Kalergis, A.M. Current and Emerging Pharmacological Treatments for Respiratory Syncytial Virus Infection in High-Risk Infants. *Expert Opinion on Pharmacotherapy* **2023**, 14656566.2023.2213433, doi:10.1080/14656566.2023.2213433.
18. World Health Organization Respiratory Syncytial Virus (RSV) Disease.
19. Acosta, P.L.; Caballero, M.T.; Polack, F.P. Brief History and Characterization of Enhanced Respiratory Syncytial Virus Disease. *Clin Vaccine Immunol* **2016**, *23*, 189–195, doi:10.1128/CVI.00609-15.
20. Murphy, B.R.; Prince, G.A.; Walsh, E.E.; Kim, H.W.; Parrott, R.H.; Hemming, V.G.; Rodriguez, W.J.; Chanock, R.M. Dissociation between Serum Neutralizing and Glycoprotein Antibody Responses of Infants and Children Who Received Inactivated Respiratory Syncytial Virus Vaccine. *J Clin Microbiol* **1986**, *24*, 197–202, doi:10.1128/jcm.24.2.197-202.1986.
21. Openshaw, P.J.M.; Chiu, C.; Culley, F.J.; Johansson, C. Protective and Harmful Immunity to RSV Infection. *Annu. Rev. Immunol.* **2017**, *35*, 501–532, doi:10.1146/annurev-immunol-051116-052206.
22. Johnson, K.M.; Bloom, H.H.; Mufson, M.A.; Chanock, R.M. Natural Reinfection of Adults by Respiratory Syncytial Virus. Possible Relation to Mild Upper Respiratory Disease. *N Engl J Med* **1962**, *267*, 68–72, doi:10.1056/NEJM196207122670204.
23. Kolli, D.; Bao, X.; Casola, A. Human Metapneumovirus Antagonism of Innate Immune Responses. *Viruses* **2012**, *4*, 3551–3571, doi:10.3390/v4123551.
24. Velayutham, T.S.; Ivanciuc, T.; Garofalo, R.P.; Casola, A. Role of Human Metapneumovirus Glycoprotein G in Modulation of Immune Responses. *Front. Immunol.* **2022**, *13*, 962925, doi:10.3389/fimmu.2022.962925.
25. Groen, K.; van Nieuwkoop, S.; Lamers, M.M.; Fouchier, R.A.M.; van den Hoogen, B.G. Evidence against the Human Metapneumovirus G, SH, and M2-2 Proteins as Bona Fide Interferon Antagonists. *J Virol* **2022**, *96*, e00723-22, doi:10.1128/jvi.00723-22.
26. González, A.E.; Lay, M.K.; Jara, E.L.; Espinoza, J.A.; Gómez, R.S.; Soto, J.; Rivera, C.A.; Abarca, K.; Bueno, S.M.; Riedel, C.A.; et al. Aberrant T Cell Immunity Triggered by Human Respiratory Syncytial Virus and Human Metapneumovirus Infection. *Virulence* **2017**, *8*, 685–704, doi:10.1080/21505594.2016.1265725.
27. Barik, S. Respiratory Syncytial Virus Mechanisms to Interfere with Type 1 Interferons. *Curr Top Microbiol Immunol* **2013**, *372*, 173–191, doi:10.1007/978-3-642-38919-1_9.
28. PATH *RSV Clinical Trial Tracker*;
29. PATH RSV Vaccine and MAb Snapshot Available online: https://www.path.org/resources/rsv-vaccine-and-mab-snapshot/.
30. Scotta, M.C.; Stein, R.T. Current Strategies and Perspectives for Active and Passive Immunization against Respiratory Syncytial Virus in Childhood. *Jornal de Pediatria* **2023**, *99*, S4–S11, doi:10.1016/j.jped.2022.10.004.
31. Vidal Valero, M. "A Good Day": FDA Approves World's First RSV Vaccine. *Nature* **2023**, *617*, 234–235, doi:10.1038/d41586-023-01529-5.
32. Papi, A.; Ison, M.G.; Langley, J.M.; Lee, D.-G.; Leroux-Roels, I.; Martinon-Torres, F.; Schwarz, T.F.; Van Zyl-Smit, R.N.; Campora, L.; Dezutter, N.; et al. Respiratory Syncytial Virus Prefusion F Protein Vaccine in Older Adults. *N Engl J Med* **2023**, *388*, 595–608, doi:10.1056/NEJMoa2209604.

33. Karron, R.A.; Buchholz, U.J.; Collins, P.L. Live-Attenuated Respiratory Syncytial Virus Vaccines. In *Challenges and Opportunities for Respiratory Syncytial Virus Vaccines*; Anderson, L.J., Graham, B.S., Eds.; Current Topics in Microbiology and Immunology; Springer Berlin Heidelberg: Berlin, Heidelberg, 2013; Vol. 372, pp. 259–284 ISBN 978-3-642-38918-4.
34. Anderson, L.J.; Dormitzer, P.R.; Nokes, D.J.; Rappuoli, R.; Roca, A.; Graham, B.S. Strategic Priorities for Respiratory Syncytial Virus (RSV) Vaccine Development. *Vaccine* **2013**, *31 Suppl 2*, B209-215, doi:10.1016/j.vaccine.2012.11.106.
35. Luongo, C.; Winter, C.C.; Collins, P.L.; Buchholz, U.J. Respiratory Syncytial Virus Modified by Deletions of the NS2 Gene and Amino Acid S1313 of the L Polymerase Protein Is a Temperature-Sensitive, Live-Attenuated Vaccine Candidate That Is Phenotypically Stable at Physiological Temperature. *J Virol* **2013**, *87*, 1985–1996, doi:10.1128/JVI.02769-12.
36. Cunningham, C.K.; Karron, R.; Muresan, P.; McFarland, E.J.; Perlowski, C.; Libous, J.; Thumar, B.; Gnanashanmugam, D.; Moye, J.; Schappell, E.; et al. Live-Attenuated Respiratory Syncytial Virus Vaccine With Deletion of RNA Synthesis Regulatory Protein M2-2 and Cold Passage Mutations Is Overattenuated. *Open Forum Infectious Diseases* **2019**, *6*, ofz212, doi:10.1093/ofid/ofz212.
37. Karron, R.A.; Luongo, C.; Mateo, J.S.; Wanionek, K.; Collins, P.L.; Buchholz, U.J. Safety and Immunogenicity of the Respiratory Syncytial Virus Vaccine RSV/ΔNS2/Δ1313/I1314L in RSV-Seronegative Children. *The Journal of Infectious Diseases* **2020**, *222*, 82–91, doi:10.1093/infdis/jiz408.
38. Verdijk, P.; van der Plas, J.L.; van Brummelen, E.M.J.; Jeeninga, R.E.; de Haan, C.A.M.; Roestenberg, M.; Burggraaf, J.; Kamerling, I.M.C. First-in-Human Administration of a Live-Attenuated RSV Vaccine Lacking the G-Protein Assessing Safety, Tolerability, Shedding and Immunogenicity: A Randomized Controlled Trial. *Vaccine* **2020**, *38*, 6088–6095, doi:10.1016/j.vaccine.2020.07.029.
39. McFarland, E.J.; Karron, R.A.; Muresan, P.; Cunningham, C.K.; Libous, J.; Perlowski, C.; Thumar, B.; Gnanashanmugam, D.; Moye, J.; Schappell, E.; et al. Live Respiratory Syncytial Virus Attenuated by M2-2 Deletion and Stabilized Temperature Sensitivity Mutation 1030s Is a Promising Vaccine Candidate in Children. *The Journal of Infectious Diseases* **2020**, *221*, 534–543, doi:10.1093/infdis/jiz603.
40. Cunningham, C.K.; Karron, R.A.; Muresan, P.; Kelly, M.S.; McFarland, E.J.; Perlowski, C.; Libous, J.; Oliva, J.; Jean-Philippe, P.; Moye, J.; et al. Evaluation of Recombinant Live-Attenuated Respiratory Syncytial Virus (RSV) Vaccines RSV/ΔNS2/Δ1313/I1314L and RSV/276 in RSV-Seronegative Children. *The Journal of Infectious Diseases* **2022**, *226*, 2069–2078, doi:10.1093/infdis/jiac253.
41. Karron, R.A.; Atwell, J.E.; McFarland, E.J.; Cunningham, C.K.; Muresan, P.; Perlowski, C.; Libous, J.; Spector, S.A.; Yogev, R.; Aziz, M.; et al. Live-Attenuated Vaccines Prevent Respiratory Syncytial Virus–Associated Illness in Young Children. *Am J Respir Crit Care Med* **2021**, *203*, 594–603, doi:10.1164/rccm.202005-1660OC.
42. Stobart, C.C.; Rostad, C.A.; Ke, Z.; Dillard, R.S.; Hampton, C.M.; Strauss, J.D.; Yi, H.; Hotard, A.L.; Meng, J.; Pickles, R.J.; et al. A Live RSV Vaccine with Engineered Thermostability Is Immunogenic in Cotton Rats despite High Attenuation. *Nat Commun* **2016**, *7*, 13916, doi:10.1038/ncomms13916.
43. Meissa Vaccines, Inc. *Study of the Safety and Immunogenicity of an Intranasal Vaccine for Respiratory Syncytial Virus in Seropositive Children (NCT04444284)*; 2021;
44. Meissa Vaccines, Inc. *Safety and Immunogenicity of an Intranasal Vaccine for Respiratory Syncytial Virus in Seronegative Children 6-36 Months (NCT04909021)*; 2022;
45. National Institute of Allergy and Infectious Diseases (NIAID) *Evaluating the Infectivity, Safety, and Immunogenicity of Recombinant Live-Attenuated RSV Vaccines RSV ΔNS2/Δ1313/I1314L or RSV 276 in RSV-Seronegative Infants 6 to 24 Months of Age (NCT03227029)*; 2022;

46. National Institute of Allergy and Infectious Diseases (NIAID) *Safety and Immunogenicity of a Single Dose of the Recombinant Live-Attenuated Respiratory Syncytial Virus (RSV) Vaccines RSV ΔNS2/Δ1313/I1314L, RSV 6120/ΔNS2/1030s, RSV 276 or Placebo, Delivered as Nose Drops to RSV-Seronegative Children 6 to 24 Months of Age (NCT03916185)*; 2022;
47. Biacchesi, S.; Skiadopoulos, M.H.; Yang, L.; Lamirande, E.W.; Tran, K.C.; Murphy, B.R.; Collins, P.L.; Buchholz, U.J. Recombinant Human Metapneumovirus Lacking the Small Hydrophobic SH and/or Attachment G Glycoprotein: Deletion of G Yields a Promising Vaccine Candidate. *J Virol* **2004**, *78*, 12877–12887, doi:10.1128/JVI.78.23.12877-12887.2004.
48. Biacchesi, S.; Pham, Q.N.; Skiadopoulos, M.H.; Murphy, B.R.; Collins, P.L.; Buchholz, U.J. Infection of Nonhuman Primates with Recombinant Human Metapneumovirus Lacking the SH, G, or M2-2 Protein Categorizes Each as a Nonessential Accessory Protein and Identifies Vaccine Candidates. *J Virol* **2005**, *79*, 12608–12613, doi:10.1128/JVI.79.19.12608-12613.2005.
49. Márquez-Escobar, V.A. Current Developments and Prospects on Human Metapneumovirus Vaccines. *Expert Review of Vaccines* **2017**, *16*, 419–431, doi:10.1080/14760584.2017.1283223.
50. Dubois, J.; Pizzorno, A.; Cavanagh, M.-H.; Padey, B.; Nicolas de Lamballerie, C.; Uyar, O.; Venable, M.-C.; Carbonneau, J.; Traversier, A.; Julien, T.; et al. Strain-Dependent Impact of G and SH Deletions Provide New Insights for Live-Attenuated HMPV Vaccine Development. *Vaccines* **2019**, *7*, 164, doi:10.3390/vaccines7040164.
51. Chupin, C.; Pizzorno, A.; Traversier, A.; Brun, P.; Ogonczyk-Makowska, D.; Padey, B.; Milesi, C.; Dulière, V.; Laurent, E.; Julien, T.; et al. Avian Cell Line DuckCelt®-T17 Is an Efficient Production System for Live-Attenuated Human Metapneumovirus Vaccine Candidate Metavac®. *Vaccines* **2021**, *9*, 1190, doi:10.3390/vaccines9101190.
52. Lê, V.B.; Dubois, J.; Couture, C.; Cavanagh, M.-H.; Uyar, O.; Pizzorno, A.; Rosa-Calatrava, M.; Hamelin, M.-È.; Boivin, G. Human Metapneumovirus Activates NOD-like Receptor Protein 3 Inflammasome via Its Small Hydrophobic Protein Which Plays a Detrimental Role during Infection in Mice. *PLoS Pathog* **2019**, *15*, e1007689, doi:10.1371/journal.ppat.1007689.
53. Aerts, L.; Cavanagh, M.-H.; Dubois, J.; Carbonneau, J.; Rhéaume, C.; Lavigne, S.; Couture, C.; Hamelin, M.-È.; Boivin, G. Effect of In Vitro Syncytium Formation on the Severity of Human Metapneumovirus Disease in a Murine Model. *PLoS ONE* **2015**, *10*, e0120283, doi:10.1371/journal.pone.0120283.
54. Dubois, J.; Cavanagh, M.-H.; Terrier, O.; Hamelin, M.-È.; Lina, B.; Shi, R.; Rosa-Calatrava, M.; Boivin, G. Mutations in the Fusion Protein Heptad Repeat Domains of Human Metapneumovirus Impact on the Formation of Syncytia. *Journal of General Virology* **2017**, *98*, 1174–1180, doi:10.1099/jgv.0.000796.
55. García, J.; García-Barreno, B.; Vivo, A.; Melero, J.A. 241. *Virology* **1993**, *195*, 243–247, doi:10.1006/viro.1993.1366.
56. Derdowski, A.; Peters, T.R.; Glover, N.; Qian, R.; Utley, T.J.; Burnett, A.; Williams, J.V.; Spearman, P.; Crowe, J.E. Human Metapneumovirus Nucleoprotein and Phosphoprotein Interact and Provide the Minimal Requirements for Inclusion Body Formation. *Journal of General Virology* **2008**, *89*, 2698–2708, doi:10.1099/vir.0.2008/004051-0.
57. Zhou, M.; Kitagawa, Y.; Yamaguchi, M.; Uchiyama, C.; Itoh, M.; Gotoh, B. Expeditious Neutralization Assay for Human Metapneumovirus Based on a Recombinant Virus Expressing Renilla Luciferase. *Journal of Clinical Virology* **2013**, *56*, 31–36, doi:10.1016/j.jcv.2012.09.014.
58. Biacchesi, S.; Skiadopoulos, M.H.; Tran, K.C.; Murphy, B.R.; Collins, P.L.; Buchholz, U.J. Recovery of Human Metapneumovirus from CDNA: Optimization of Growth in Vitro and Expression of Additional Genes. *Virology* **2004**, *321*, 247–259, doi:10.1016/j.virol.2003.12.020.
59. De Graaf, M.; Herfst, S.; Schrauwen, E.J.A.; Van Den Hoogen, B.G.; Osterhaus, A.D.M.E.; Fouchier, R.A.M. An Improved Plaque Reduction Virus Neutralization Assay for Human Metapneumovirus. *Journal of Virological Methods* **2007**, *143*, 169–174, doi:10.1016/j.jviromet.2007.03.005.

60. Ogonczyk Makowska, D.; Hamelin, M.-È.; Boivin, G. Engineering of Live Chimeric Vaccines against Human Metapneumovirus. *Pathogens* **2020**, *9*, 135, doi:10.3390/pathogens9020135.
61. Skiadopoulos, M.H.; Surman, S.R.; Durbin, A.P.; Collins, P.L.; Murphy, B.R. Long Nucleotide Insertions between the HN and L Protein Coding Regions of Human Parainfluenza Virus Type 3 Yield Viruses With Temperature-Sensitive and Attenuation Phenotypes. *Virology* **2000**, *272*, 225–234, doi:10.1006/viro.2000.0372.
62. Schmidt, A.C.; McAuliffe, J.M.; Murphy, B.R.; Collins, P.L. Recombinant Bovine/Human Parainfluenza Virus Type 3 (B/HPIV3) Expressing the Respiratory Syncytial Virus (RSV) G and F Proteins Can Be Used To Achieve Simultaneous Mucosal Immunization against RSV and HPIV3. *J. Virol.* **2001**, *75*, 4594–4603, doi:10.1128/JVI.75.10.4594-4603.2001.
63. Liang, B.; Munir, S.; Amaro-Carambot, E.; Surman, S.; Mackow, N.; Yang, L.; Buchholz, U.J.; Collins, P.L.; Schaap-Nutt, A. Chimeric Bovine/Human Parainfluenza Virus Type 3 Expressing Respiratory Syncytial Virus (RSV) F Glycoprotein: Effect of Insert Position on Expression, Replication, Immunogenicity, Stability, and Protection against RSV Infection. *Journal of Virology* **2014**, *88*, 4237–4250, doi:10.1128/JVI.03481-13.
64. Ikegame, S.; Hashiguchi, T.; Hung, C.-T.; Dobrindt, K.; Brennand, K.J.; Takeda, M.; Lee, B. Fitness Selection of Hyperfusogenic Measles Virus F Proteins Associated with Neuropathogenic Phenotypes. *Proc. Natl. Acad. Sci. U.S.A.* **2021**, *118*, e2026027118, doi:10.1073/pnas.2026027118.
65. Kinder, J.T.; Moncman, C.L.; Barrett, C.; Jin, H.; Kallewaard, N.; Dutch, R.E. Respiratory Syncytial Virus and Human Metapneumovirus Infections in Three-Dimensional Human Airway Tissues Expose an Interesting Dichotomy in Viral Replication, Spread, and Inhibition by Neutralizing Antibodies. *J Virol* **2020**, *94*, e01068-20, doi:10.1128/JVI.01068-20.
66. Tristram, D.A.; Hicks, W.; Hard, R. Respiratory Syncytial Virus and Human Bronchial Epithelium. *Arch Otolaryngol Head Neck Surg* **1998**, *124*, 777–783, doi:10.1001/archotol.124.7.777.
67. Zhang, L.; Peeples, M.E.; Boucher, R.C.; Collins, P.L.; Pickles, R.J. Respiratory Syncytial Virus Infection of Human Airway Epithelial Cells Is Polarized, Specific to Ciliated Cells, and without Obvious Cytopathology. *J Virol* **2002**, *76*, 5654–5666, doi:10.1128/jvi.76.11.5654-5666.2002.
68. Wright, P.F.; Ikizler, M.R.; Gonzales, R.A.; Carroll, K.N.; Johnson, J.E.; Werkhaven, J.A. Growth of Respiratory Syncytial Virus in Primary Epithelial Cells from the Human Respiratory Tract. *J Virol* **2005**, *79*, 8651–8654, doi:10.1128/JVI.79.13.8651-8654.2005.
69. Kumagai, Y.; Takeuchi, O.; Kato, H.; Kumar, H.; Matsui, K.; Morii, E.; Aozasa, K.; Kawai, T.; Akira, S. Alveolar Macrophages Are the Primary Interferon-α Producer in Pulmonary Infection with RNA Viruses. *Immunity* **2007**, *27*, 240–252, doi:10.1016/j.immuni.2007.07.013.
70. Goritzka, M.; Makris, S.; Kausar, F.; Durant, L.R.; Pereira, C.; Kumagai, Y.; Culley, F.J.; Mack, M.; Akira, S.; Johansson, C. Alveolar Macrophage–Derived Type I Interferons Orchestrate Innate Immunity to RSV through Recruitment of Antiviral Monocytes. *Journal of Experimental Medicine* **2015**, *212*, 699–714, doi:10.1084/jem.20140825.
71. Kopf, M.; Schneider, C.; Nobs, S.P. The Development and Function of Lung-Resident Macrophages and Dendritic Cells. *Nat Immunol* **2015**, *16*, 36–44, doi:10.1038/ni.3052.
72. Lamichhane, A.; Azegamia, T.; Kiyonoa, H. The Mucosal Immune System for Vaccine Development. *Vaccine* **2014**, *32*, 6711–6723, doi:10.1016/j.vaccine.2014.08.089.
73. Habibi, M.S.; Jozwik, A.; Makris, S.; Dunning, J.; Paras, A.; DeVincenzo, J.P.; de Haan, C.A.M.; Wrammert, J.; Openshaw, P.J.M.; Chiu, C. Impaired Antibody-Mediated Protection and Defective IgA B-Cell Memory in Experimental Infection of Adults with Respiratory Syncytial Virus. *Am J Respir Crit Care Med* **2015**, *191*, 1040–1049, doi:10.1164/rccm.201412-2256OC.

74. Sheikh-Mohamed, S.; Sanders, E.C.; Gommerman, J.L.; Tal, M.C. Guardians of the Oral and Nasopharyngeal Galaxy: IgA and Protection against SARS-CoV-2 Infection. *Immunol Rev* **2022**, *309*, 75–85, doi:10.1111/imr.13118.
75. Whitsett, J.A.; Alenghat, T. Respiratory Epithelial Cells Orchestrate Pulmonary Innate Immunity. *Nat Immunol* **2015**, *16*, 27–35, doi:10.1038/ni.3045.
76. Taylor, H.P.; Dimmock, N.J. Mechanism of Neutralization of Influenza Virus by Secretory IgA Is Different from That of Monomeric IgA or IgG. *J Exp Med* **1985**, *161*, 198–209, doi:10.1084/jem.161.1.198.
77. Corthésy, B. Multi-Faceted Functions of Secretory IgA at Mucosal Surfaces. *Front Immunol* **2013**, *4*, 185, doi:10.3389/fimmu.2013.00185.
78. Mouro, V.; Fischer, A. Dealing with a Mucosal Viral Pandemic: Lessons from COVID-19 Vaccines. *Mucosal Immunology* **2022**, *15*, 584–594, doi:10.1038/s41385-022-00517-8.
79. Hennings, V.; Thörn, K.; Albinsson, S.; Lingblom, C.; Andersson, K.; Andersson, C.; Järbur, K.; Pullerits, R.; Idorn, M.; Paludan, S.R.; et al. The Presence of Serum Anti-SARS-CoV-2 IgA Appears to Protect Primary Health Care Workers from COVID-19. *Eur J Immunol* **2022**, *52*, 800–809, doi:10.1002/eji.202149655.
80. Leroux-Roels, I.; Davis, M.G.; Steenackers, K.; Essink, B.; Vandermeulen, C.; Fogarty, C.; Andrews, C.P.; Kerwin, E.; David, M.-P.; Fissette, L.; et al. Safety and Immunogenicity of a Respiratory Syncytial Virus Prefusion F (RSVPreF3) Candidate Vaccine in Older Adults: Phase 1/2 Randomized Clinical Trial. *The Journal of Infectious Diseases* **2023**, *227*, 761–772, doi:10.1093/infdis/jiac327.
81. McLellan, J.S.; Chen, M.; Leung, S.; Graepel, K.W.; Du, X.; Yang, Y.; Zhou, T.; Baxa, U.; Yasuda, E.; Beaumont, T.; et al. Structure of RSV Fusion Glycoprotein Trimer Bound to a Prefusion-Specific Neutralizing Antibody. *Science* **2013**, *340*, 1113–1117, doi:10.1126/science.1234914.
82. Liang, B.; Surman, S.; Amaro-Carambot, E.; Kabatova, B.; Mackow, N.; Lingemann, M.; Yang, L.; McLellan, J.S.; Graham, B.S.; Kwong, P.D.; et al. Enhanced Neutralizing Antibody Response Induced by Respiratory Syncytial Virus Prefusion F Protein Expressed by a Vaccine Candidate. *J Virol* **2015**, *89*, 9499–9510, doi:10.1128/JVI.01373-15.
83. Liang, B.; Ngwuta, J.O.; Herbert, R.; Swerczek, J.; Dorward, D.W.; Amaro-Carambot, E.; Mackow, N.; Kabatova, B.; Lingemann, M.; Surman, S.; et al. Packaging and Prefusion Stabilization Separately and Additively Increase the Quantity and Quality of Respiratory Syncytial Virus (RSV)-Neutralizing Antibodies Induced by an RSV Fusion Protein Expressed by a Parainfluenza Virus Vector. *J Virol* **2016**, *90*, 10022–10038, doi:10.1128/JVI.01196-16.
84. Ngwuta, J.O.; Chen, M.; Modjarrad, K.; Joyce, M.G.; Kanekiyo, M.; Kumar, A.; Yassine, H.M.; Moin, S.M.; Killikelly, A.M.; Chuang, G.-Y.; et al. Prefusion F–Specific Antibodies Determine the Magnitude of RSV Neutralizing Activity in Human Sera. *Sci. Transl. Med.* **2015**, *7*, doi:10.1126/scitranslmed.aac4241.
85. Blanco, J.C.G.; Pletneva, L.M.; McGinnes-Cullen, L.; Otoa, R.O.; Patel, M.C.; Fernando, L.R.; Boukhvalova, M.S.; Morrison, T.G. Efficacy of a Respiratory Syncytial Virus Vaccine Candidate in a Maternal Immunization Model. *Nat Commun* **2018**, *9*, 1904, doi:10.1038/s41467-018-04216-6.
86. Crank, M.C.; Ruckwardt, T.J.; Chen, M.; Morabito, K.M.; Phung, E.; Costner, P.J.; Holman, L.A.; Hickman, S.P.; Berkowitz, N.M.; Gordon, I.J.; et al. A Proof of Concept for Structure-Based Vaccine Design Targeting RSV in Humans. *Science* **2019**, *365*, 505–509, doi:10.1126/science.aav9033.
87. Chang, L.A.; Phung, E.; Crank, M.C.; Morabito, K.M.; Villafana, T.; Dubovsky, F.; Falloon, J.; Esser, M.T.; Lin, B.C.; Chen, G.L.; et al. A Prefusion-Stabilized RSV F Subunit Vaccine Elicits B Cell Responses with Greater Breadth and Potency than a Postfusion F Vaccine. *Sci. Transl. Med.* **2022**, *14*, eade0424, doi:10.1126/scitranslmed.ade0424.
88. Morens, D.M.; Taubenberger, J.K.; Fauci, A.S. Rethinking Next-Generation Vaccines for Coronaviruses, Influenzaviruses, and Other Respiratory Viruses. *Cell Host & Microbe* **2023**, *31*, 146–157, doi:10.1016/j.chom.2022.11.016.
89. Shi, S.; Zhu, H.; Xia, X.; Liang, Z.; Ma, X.; Sun, B. Vaccine Adjuvants: Understanding the Structure and Mechanism of Adjuvanticity. *Vaccine* **2019**, *37*, 3167–3178, doi:10.1016/j.vaccine.2019.04.055.

90. Rameix-Welti, M.-A.; Le Goffic, R.; Hervé, P.-L.; Sourimant, J.; Rémot, A.; Riffault, S.; Yu, Q.; Galloux, M.; Gault, E.; Eléouët, J.-F. Visualizing the Replication of Respiratory Syncytial Virus in Cells and in Living Mice. *Nat Commun* **2014**, *5*, 5104, doi:10.1038/ncomms6104.

Supplementary figures

Supplementary figure 1

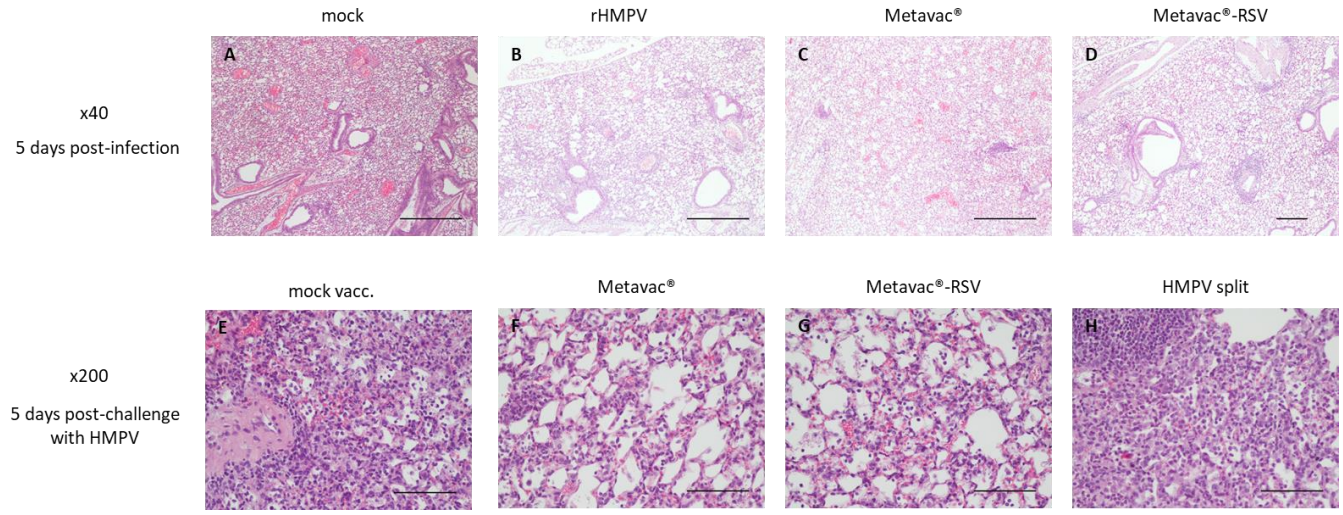

Histopathological lung studies from infected (panels A-D) or vaccinated then challenged (panels E-H) mice.
40-fold magnified histopathological images of lung tissues 5 days post-infection: (A) Normal lung parenchyma in mock-infected animal. (B) Intranasal (IN) infection with rHMPV virus resulted in mild to moderate peri-bronchial and peri-vascular inflammation. (C) IN infection with monovalent Metavac® LAV candidate resulted in mild interstitial, peri-bronchial and perivascular inflammation. (D) IN infection with bivalent Metavac®-RSV LAV candidate resulted in mild interstitial, peri-bronchial and perivascular inflammation. Scale bar = 500µm.
200-fold magnified histopathological images of lung tissues 5 days post-challenge with HMPV: (A) Normal lung parenchyma in mock-infected animal. (E) Interstitial inflammation with alveolar wall thickening and intra-alveolar inflammatory cells (neutrophils, macrophages) in infected non-vaccinated mice. (F-G) Dual IN immunisation with monovalent Metavac® (F) or bivalent Metavac®-RSV (G) vaccine candidates and HMPV challenge resulted in mild (interstitial inflammation. (H) Dual IM immunisation with split inactivated HMPV preparation and HMPV challenge resulted in moderate to marked peri-bronchial inflammation, moderate interstitial inflammation, focal pleural inflammation and marked peri-vascular inflammation. Scale bar = 100µm.

Supplementary figure 2

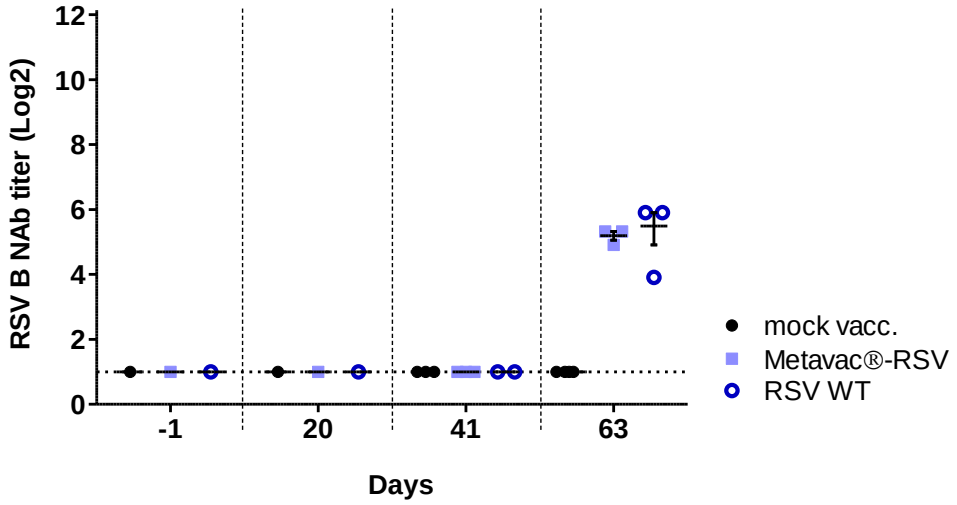

Neutralisation studies for heterologous RSV B strain. To evaluate the production of specific neutralizing antibody response against heterologous virus strains, sera were recovered from blood samples, pooled and heat-inactivated at 56°C until testing. Serial twofold dilutions of sera in infection medium were then tested for neutralization of RSV B strain WV/14617/85 (VR-1400™, ATCC) on Vero cells. Reciprocal neutralizing antibody (NAb) titers were determined by an endpoint dilution assay based on CPEs observation.